ANNALS OF PHYSICS 206, 440–493 (1991)

Adiabatic Quantum Transport in Networks with Macroscopic Components

J. E. AVRON

Department of Physics, Technion, Hafia 32000, Israel

AND

L. SADUN

Courant Institute of Mathematical Sciences, New York University, New York, New York 10012

Received June 4, 1990

We study the Chern numbers associated with the quantum adiabatic conductances in networks that have mesoscopic and macroscopic components. The classes of networks considered have links that are single-mode electron wave-guides, with commensurate lengths, and three independent flux tubes that thread three loops. The mesoscopic part of the networks have few vertices and the macroscopic parts are made of few long leads or long loops. For such networks the analysis of the Schrödinger operator reduces to the study of small matrices. We analyse various classes of such networks qualitatively and solve explicitly a representative model in each class. We find two scenarios that are the analogs of the integer and classical Hall effects. In particular, the adiabatic transport at zero temperature for noninteracting Fermions, is an integer in one scenario and a real (i.e., non-integer) number, in the other. We also discuss an interpretation of the results in terms of the scattering data. This leads to Landauer type formulas for adiabatic transport.

CONTENTS

0003-4916/91 $7.50

1. INTRODUCTION

In this work we study the geometric aspects of quantum adiabatic conductance in multiply connected systems that contain both mesoscopic and macroscopic components.

A. *Background*

A network is represented by a graph whose loops are threaded by independent, externally controllable, flux tubes ϕ_i. We shall consider networks with three flux tubes, ϕ_1, ϕ_2, and ϕ_3, which turn out to be the simplest nontrivial cases. See, e.g., Fig. 1. The electrons are constrained to the links of the graph, and their dynamics are governed by the appropriate Schrödinger equation. We consider links that are "one mode electron wave guides." The electron dynamics are then governed by the one-dimensional Schrödinger equation with boundary conditions at the vertices. (The multimode situation corresponds to the one-dimensional vector-valued Schrödinger equation.)

The basic question we address is the following: Suppose that initially the system is in an eigenstate and the flux ϕ_j is increased adiabatically by the unit of quantum flux. What is the charge transported around loop i? (We choose units where the flux quantum is 2π.)

Since the initial and final Hamiltonians of the system are related by a gauge transformation, in the absence of level crossings, the initial and final states must also be related by the same gauge transformation, and so the initial and final charge densities are the same. An argument, due to Laughlin [1] suggests that in such circumstances the charge transported around loop i is an integer. This argument does not always hold for mesoscopic systems because the electronic wave function

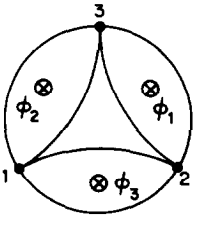

FIG. 1. The mesoscopic hubcap, threated by three independent fluxes.

may be extended throughout the system. However, the average over ϕ_i of this charge is known to always be an integer provided the corresponding eigenstate is nondegenerate for all ϕ_i and ϕ_j [2, 3]. In fact, there are no power corrections to the integer in the adiabatic expansion [4]. We call this integer the conductance and denote it g_{ij}.

The integer g_{ij} is the Chern number of the eigenstate bundle at fixed value of the remaining flux ϕ_k, and may be thought of as a topological quantum number. It is both periodic and antisymmetric as a function of φ_k:

$$g_{ij}(\phi_k + 2\pi) = g_{ij}(\phi_k). \tag{1.1}$$

$$g_{ij}(\phi_k) = -g_{ij}(-\phi_k). \tag{1.2}$$

Being integer valued, $g_{ij}(\phi_k)$ can only change discontinuously. These discontinuities occur at those values of ϕ_k where level crossings occur (for *some* ϕ_i and ϕ_j).

The basic geometric ideas go back to the quantum Hall effect, where there is an extensive literature that examines the Hall conductance from a differential geometric viewpoint [5–20]. A study in the context of isolated mesoscopic systems was made in [21]. The present work is as a continuation of this program. Partial results were announced in [22].

B. *Networks with Macroscopic Components*

In this paper we study the conductances of isolated mesoscopic networks with a few macroscopic components. More specifically, we consider networks with one or more macroscopic leads or loops. We have been motivated in part by recent experiments and theoretical work on mesoscopic systems (See [23] for a review) and more specifically by the question: How do leads affect transport phenomena in mesoscopic systems?

Another, more theoretical, motivation is the study of Chern numbers that arise for various classes of Schrödinger operators. This is part of the program, discussed above, that started with the quantum Hall effect.

With macroscopic elements of length l, the one-electron Schrödinger equation has $O(l)$ eigenstates in each energy interval of size $O(1)$, so there are very many Chern numbers to compute. For noninteracting electrons with a given density at temperature T, the (averaged) conductance is the sum, over states, of the Chern number of each eigenstate times its occupation probability. In particular, at $T=0$ the conductance is the sum of the Chern numbers of all the states below the Fermi energy.

This physical interpretation of the weighted sum of Chern numbers as low temperature conductances assumes that the order of limits is as follows: The adiabatic limit is taken first, then the macroscopic limit $l \to \infty$, and finally the low temperature limit $T \to 0$. While it is of interest to take the limits in different orders, and in particular to take the $l \to \infty$ first, such analysis is outside the scope of this work. We also note that there may be avoided crossings on a small energy scale (see, e.g., [24]), so insisting on taking the adiabatic limit first is a strong condition.

Our purpose is both to develop methods for computing Chern numbers for large l and to understand some of the qualitative features of the low temperature conductances. The networks we consider are connected, and contain both macroscopic and mesoscopic components. We examine only those classes of networks whose links have commensurate lengths. Incommensurate networks form a class to themselves, outside the scope of the present work. Under these circumstances the qualitative patterns of the Chern numbers fall into one of the following scenarios:

(a) The *integer* scenario. The integer scenario is an analog of the integer Hall effect. The conductance of noninteracting electrons with fixed density has a well-defined *integer* limit as $l \to \infty$ and has wide plateaus (i.e., regions of constant value of length $O(1)$) as functions of the Fermi energy or the controlling flux. The plateaus are separated by sharp integer jumps.

On a microscopic level, all but a handful ($O(1)$ in a given energy interval) of the states have $g_{ij} = 0$ for any given value ϕ_k of the controlling flux. In particular, the conductance is carried by few states that may lie deep below the Fermi energy. The wide plateaus come about through an interesting mechanism. As we vary, e.g., ϕ_3, there are usually lots ($O(l)$) of level crossings among the single particle states that transfer a nonzero conductance from one level to a neighboring one. Such crossings, however, do not affect the conductance of the multielectron system as long as the crossing is between two states that are both occupied (i.e., below the Fermi energy) or both unoccupied. Only at special values of ϕ_3 (typically $O(1)$ apart), where the level crossing is *at* the Fermi surface, does the conductance of the multielectron system change. We shall refer to this mechanism as the *bucket brigade*.

This scenario occurs typically when a single macroscopic component is attached to a mesoscopic network. An intuition to this is the (almost) disconnected network, Fig. 5. Unless a state satisfies a resonant condition, it will be supported almost entirely away from the fluxes. Such a state cannot transport an integer number of electrons around the loops as the fluxes are varied, and so it will not conduct. Only a few states, spaced $O(1)$ apart, which satisfy a resonant condition and so have large amplitudes on the network, can have a non-zero Chern number.

The integer scenario also occurs in networks with a macroscopic loop that is used to drive the network, for more complicated reasons.

(b) The *real* scenario. The real scenario is an analog of the classical Hall effect where the Hall conductance is not quantized. The low temperature conductance of the multiparticle system has a well-defined *real* limit as $l \to \infty$ (we take the $l \to \infty$ limit *before* taking the limit $T \to 0$). There are no strict plateaus, but, as we shall see, there still are sharp jumps of size $O(1)$ in the conductance that are spaced $O(1)$ apart.

On a microscopic level, many, that is $O(l)$, of the one particle states in a given energy interval have non-zero Chern numbers. The conductance, a sum of Chern

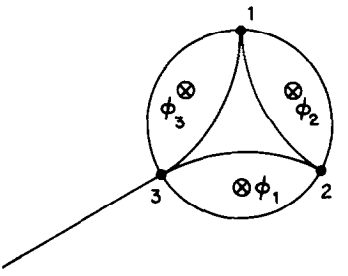

FIG. 2. The mesoscopic hubcap with a macroscopic lead.

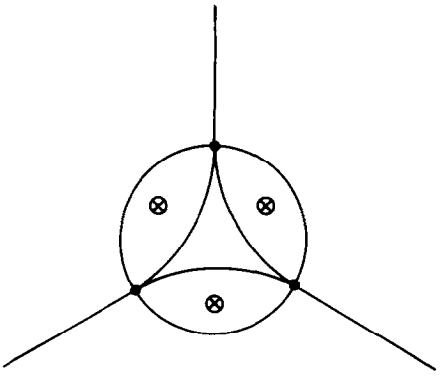

FIG. 3. The mesoscopic hubcap with three macroscopic leads.

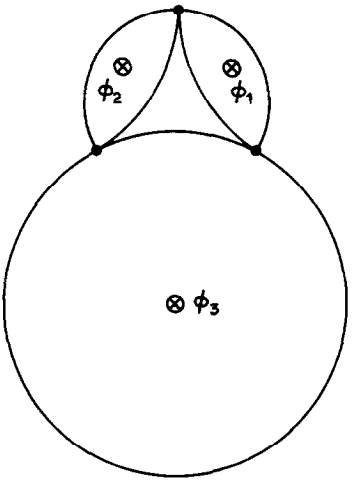

FIG. 4. The mesoscopic hubcap with a macroscopic loop.

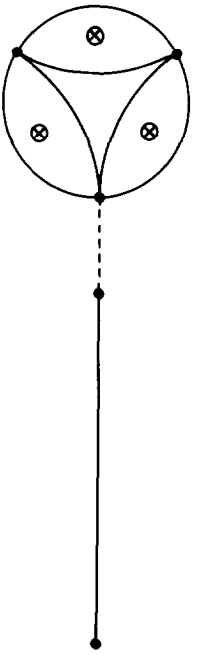

FIG. 5. A mesoscopic hubcap with a disconnected, or weakly coupled macroscopic lead.

numbers times occupation probabilities, need not be an integer, since for any T there will be many conducting states near the Fermi energy for l large enough.

The real scenario occurs, typically, in networks with several macroscopic components. In particular this is the case in networks with as many leads as vertices. These have the additional feature that the Chern numbers repeat periodically, with $O(l)$ periods in energy intervals of $O(1)$. It is also observed in the conductance of networks with one large loop that is threaded by the "controlling" flux ϕ_k. There is no observed scenario that is an analog of the fractional quantum Hall effect.

In both scenarios the conductances and the Chern numbers that arise are $O(1)$, even though there is a large parameter in the problem, l. This is in contrast with the Hall effect for a periodic crystal where large Chern numbers are known to occur with appropriate choices of the flux through the unit cell [7, 10, 11, 25].

Our methods of analysis are general. However, as examples we consider the networks of Figs. 2–4, all of which are a variation on Fig. 1, the "hubcap."

C. *Acknowledgments*

The bulk of this work was done at Caltech, and we thank B. Simon and M. Cross for their hospitality. J.E.A. thanks the Aspen Center for Physics and D. Mukamel for the hospitality at the Einstein center at the Weizmann Institute, where parts of this work were done. We thank J. Segert for helpful discussions. This work is supported in part by the BSF under Grant 88-00325, by the Israel Academy of Sciences Grant 1380021, and by the NSF Grant DMS-8806731.

2. The Spectral Matrix

The spectral analysis of Schrödinger operators associated with networks is a subject of long history that goes back to the 1950s [26]. For the reader's convenience we recall here how Schrödinger equations associated with networks are formulated and how their spectral analysis reduces to studying finite-dimensional matrices [26–30, 52, 53]. We further describe networks with leads and loops. A detailed analysis of the special cases where the reduction fails is included in the Appendix.

A. *Formulation*

The Schrödinger operator associated to a network of single mode links is defined by the one-dimensional Schrödinger equation associated to each link, together with appropriate boundary conditions at the vertices. These boundary conditions can be viewed as generalizations of boundary conditions at the ends of intervals.

In the absence of gauge fields, we consider boundary conditions at the vertex j of the form

$$\sum_l \partial_l \psi|_j = \lambda_j \psi|_j, \tag{2.1}$$

where $\partial_l \psi$ is the derivative along the lth link emanating from j, and λ_j is real. See Fig. 6. This is the only choice of boundary condition that preserves self-adjointness and is permutation symmetric with respect to the interchange of links. In analogy to the terminology for intervals, we call $\lambda_j = 0$ a Neuman boundary condition and call $\lambda_j = \infty$ a Dirichlet boundary condition.

In the presence of a gauge field A_l on the lth link, we replace (2.1) by

$$\sum_l D_l \psi|_j = \lambda_j \psi|_j, \tag{2.2}$$

where $D_l \equiv (\partial_l - iA_l)$ is the covariant derivative along link l.

B. *Ideal Electron Wave Guides*

An ideal electron wave guide is a wire (or link) l on which the potential is zero, so that the Hamiltonian associated with l is

$$H_l \equiv -\frac{1}{2m}(D_l)^2. \tag{2.3}$$

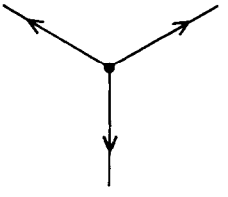

FIG. 6. A vertex where three links meet.

An ideal network is a network in which all the links are ideal wave guides. In ideal networks the spectral analysis of the Schrödinger operator reduces to a study of finite matrices. Let

$$\phi(x) \equiv \int^x A(y)\, dy, \qquad E \equiv k^2/2m, \qquad k \geqslant 0. \tag{2.4}$$

The space of solutions of $H_l\psi = E\psi$ is two dimensional and is spanned by

$$\exp(i\phi(x)) \exp(\pm ikx). \tag{2.5}$$

For an eigenfunction of energy E, we must choose the amplitudes of the right and left moving waves in (2.5) for all the links, such that at each vertex ψ is continuous and satisfies Eq. (2.2). This is clearly a matrix problem whose dimension is twice the number of links. The eigenvalue problem is to find $k(A)$, the set of all k's for which such a solution exists.

The conventional, and more useful, reduction is to a smaller matrix problem whose dimension is the number of vertices in the graph. The reduction can be done for all k's outside of a discrete set for which, for some link j of length l_j,

$$\sin(kl_j) = 0. \tag{2.6}$$

We call such k's *singular*. If all the lengths are commensurate (say, integers) then the set of singular k's is discrete and periodic. Henceforth in this chapter we will deal only with nonsingular k's. The matrix problem for k singular is treated in the Appendix.

C. *The Spectral Matrix for Simple Networks*

We call a network *simple* if each link has two distinct endpoints (i.e., does not run from a point to itself). To every simple network with n vertices we will associate an $n \times n$ *spectral matrix* $h(k, A)$, which determines all non-singular points in the spectrum $k(A)$. Specifically, a given nonsingular k is in $k(A)$ if and only if $\det h(k, A) = 0$. The construction of the spectral matrix follows:

On a link of length l with $\sin(kl) \neq 0$, the wave function on the link is determined by its values at the endpoints:

$$\psi_l(x) = \frac{\exp(i\phi(x))}{\sin(kl)} [\psi(l) \exp(-i\phi(l)) \sin(kx) + \psi(0) \sin(k(l-x))]. \tag{2.7}$$

It follows that

$$(D_l\psi)(0) = \frac{k}{\sin(kl)} [\psi(l) \exp(-i\phi(l)) - \psi(0) \cos(kl)]. \tag{2.8}$$

Substituting this into the boundary condition (2.2) for the jth vertex, we obtain

$$-\sum_{\langle ij \rangle} \cot(kl_{ij})\, \Psi_j + \sum_{\langle ij \rangle} \frac{\exp(-i\phi(l_{ij}))}{\sin(kl_{ij})}\, \Psi_i = (\lambda_j/k)\, \Psi_j, \tag{2.9}$$

where Ψ_j is the wave function amplitude at vertex i, $\langle ij \rangle$ is a link, of length l_{ij}, connecting vertices i and j, and

$$\phi(l_{ij}) \equiv \int_{\langle ij \rangle} A(x)\, dx. \tag{2.10}$$

The n equations (2.9) can be organized in a matrix form,

$$h(k, A)\Psi = 0, \tag{2.11}$$

where $\Psi = (\Psi_1, ..., \Psi_n)$ is the vector of amplitudes at the vertices and $h(k, A)$, the *spectral matrix*, is the Hermitian $n \times n$ matrix

$$\begin{aligned} h_{ij} &= \sum \frac{\exp(-i\phi(l_{ij}))}{\sin(kl_{ij})}, \qquad i \neq j \\ h_{ii} &= -\frac{\lambda_j}{k} - \sum \cot(kl_{ij}). \end{aligned} \tag{2.12}$$

The first sum in (2.12) is over all links connecting vertices i and j, while the second sum is over all links incident on i. If there is no link connecting i and j, then $h_{ij} = 0$. The basic property of the spectral matrix is:

> *The kernel of $h(k, A)$ corresponds to energy eigenstates and the multiplicity of a point in the spectrum is the corank of h. (Corank 0 means that k is not in the spectrum).*

Remarks. (a) For Neuman boundary conditions, $\lambda_j = 0$, the dependence of h on k is trigonometric. If the lengths are commensurate (say, integers), then h is periodic in k (say, with period 2π). So if k is in the spectrum, then so is $k + 2\pi$, and the eigenfunctions at these two wave numbers have the *same* amplitudes at the vertices.

(b) For a degenerate graph of one point it is convenient to define $h \equiv -\lambda/k$.

(c) $h(k, -A) = h^*(k, A) = h^{\mathrm{T}}(k, A)$, so h transforms under time-reversal like a Hamiltonian.

(d) Gauge transformations are implemented by diagonal unitary matrices. $h(k, A)$ and $h(k, A')$ are gauge equivalent if $\phi(A) - \phi(A') = 0 \bmod 2\pi$.

D. *Dangling Loops*

We next consider networks that are not simple. Suppose that a loop of length l, enclosing flux ϕ, with $\sin(kl) \neq 0$ is attached to the nth vertex of a graph, Fig. 7. The construction of the previous section is easily modified to include this case. The loop contributes twice to the sum (2.2) at vertex n, once for each end of the loop.

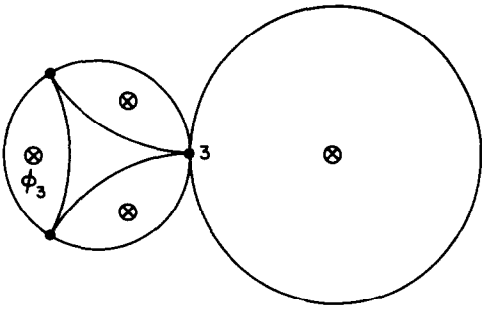

FIG. 7. The mesoscopic hubcap with a dangling loop.

By (2.8) these two contributions add up to

$$-\frac{2k}{\sin(kl)}\left[\cos(kl)-\cos(\phi)\right]\Psi_n. \tag{2.13}$$

As a result, all components of h are unchanged except for h_{nn}, to which we add

$$-2[\cos(kl)-\cos(\phi)]/\sin(kl). \tag{2.14}$$

Networks with several dangling loops have similar terms for each such loop, and as before, level crossings are determined by the rank of the spectral matrix.

E. *Networks with Leads*

Consider adding a lead of length l to the nth vertex of an n vertex graph. This creates an $n+1$ vertex graph with the associated spectral matrix. However, it is useful to keep the spectral matrix n dimensional by explicitly solving the $(n+1)$th equation,

$$\frac{\Psi_n \exp(i\phi_l)}{\sin(kl)}-\left(\frac{\lambda_{n+1}}{k}+\cot(kl)\right)\Psi_{n+1}=0, \tag{2.15}$$

for Ψ_{n+1}. This may be done so long as

$$\cot(kl)\neq -\lambda_{n+1}/k. \tag{2.16}$$

If this inequality holds we say that the lead is nonsingular. Singular leads are discussed in the Appendix.

For a nonsingular lead we solve Eq. (2.15) for Ψ_{n+1} and plug back into the other equations. This gives an $n\times n$ spectral matrix h_L for the network with the lead attached. All components of this new matrix equal those of the old matrix except for h_{nn}, to which we add the term

$$\frac{1}{\sin(kl)}\left\{-\cos(kl)+\left[\cos(kl)+\frac{\lambda_{n+1}}{k}\sin(kl)\right]^{-1}\right\}. \tag{2.16}$$

Note that when $\lambda_{n+1}=0$, (2.16) reduces to $\tan(kl)$ and

$$(h_L)_{ij}=h_{ij}+\tan(kl)\,\delta_{in}\,\delta_{jn}. \tag{2.17}$$

Adding several leads corresponds to adding several such terms.

F. *A Basic Example*

We close this chapter with an example of great importance in the sequel. We consider the mesoscopic hubcap, Fig. 1, with all the links of unit length, and all the λ's equal zero and derive the location of level crossings from the spectral matrix. We consider here only non-singular k (i.e., $\sin(k)\neq 0$); this example with k singular is treated in the Appendix.

By Eq. (2.12) the network has the spectral matrix

$$h(k, A)=[\sin(k)]^{-1}\begin{bmatrix} \alpha & 1+z & 1+\bar{y} \\ 1+\bar{z} & \alpha & 1+x \\ 1+y & 1+\bar{x} & \alpha \end{bmatrix}, \tag{2.18}$$

where

$$\alpha\equiv -4\cos(k), \qquad x\equiv\exp(i\phi_1), \qquad y\equiv\exp(i\phi_2), \qquad z\equiv\exp(i\phi_3). \tag{2.19}$$

Because of the periodicity in k and $\boldsymbol{\phi}$, it is enough to consider the basic unit cell. Since α is a monotonically increasing function of the energy for $k\in[0,\pi]$, we loosely refer to it as energy as well.

Since $h(k,\boldsymbol{\phi})$ has the form $\tilde{h}(\boldsymbol{\phi})+\alpha(k)$, the zero vector problem for h is the same as the eigenvalue problem for $\tilde{h}$, with eigenvalue $-\alpha$. Since $\tilde{h}$ has three eigenvalues, and its norm is bounded by 4, there are three energy bands with $k\in(0,\pi)$. These energy bands are shown in Fig. 8 for $\phi_1=\phi_2=\phi_3$. Since $\tilde{h}$ is traceless, these bands satisfy

$$\alpha_1(\boldsymbol{\phi})+\alpha_2(\boldsymbol{\phi})+\alpha_3(\boldsymbol{\phi})=0. \tag{2.20}$$

This means that two-level crossings with $\alpha<0$ involve the two lower levels, while crossings with $\alpha>0$ involve the two upper levels.

We find that there is one point of triple degeneracy at

$$x=y=z=-1, \qquad \alpha=0. \tag{2.21}$$

There are three points where two levels cross. The top and middle levels cross at

$$\phi_1=\phi_2=\phi_3=0, \qquad \alpha=2, \tag{2.22}$$

while the bottom and middle levels cross at

$$\phi_1=\phi_2=\phi_3=\pm 2\pi/3, \qquad \alpha=-1. \tag{2.23}$$

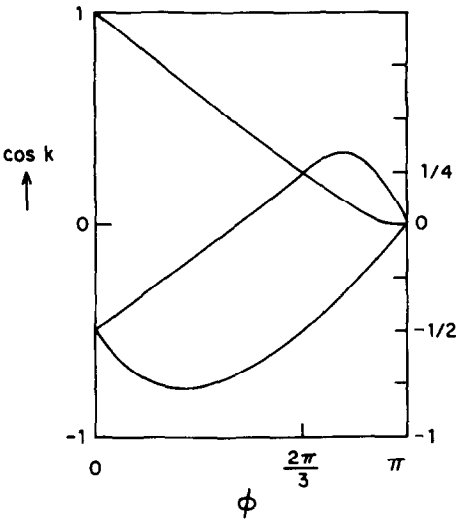

FIG. 8. The energy bands of the mesoscopic hubcap along the diagonal of the flux cube, which are the graphs of the three functions: $\alpha_1 = -(2+2\cos(\phi))$, $\alpha_2 = 1-2\cos(\phi+2\pi/3)$, and $\alpha_3 = 1-2\cos(\phi-2\pi/3)$.

This can be seen as follows: For a triple crossing h must be the zero matrix. This gives (2.21). When two levels cross h has a two-dimensional kernel, so $\operatorname{rank}(h)=1$ and all three rows are proportional. All the minors of h then vanish, implying

$$\alpha^2 = |1+x|^2 = |1+y|^2 = |1+z|^2 \tag{2.24}$$

$$\alpha^3 = \alpha\,|1+\bar{y}|^2 = (1+x)(1+y)(1+z). \tag{2.25}$$

The first equation says that either (I) $x=\bar{y}$, or (II) $x=y$, with similar relations between x and z and between y and z. In case (I), (2.25) says $\alpha = 1+z$, which forces z to be real, so $x=y=z\pm 1$ and $\alpha=0$ or 2; $\alpha=0$ corresponds to the triple degeneracy (2.21); $\alpha=2$ gives (2.22).

It remains to consider $x=y$ with either $z=\bar{y}$ or $z=y$. If $z=\bar{y}$ we recover the situation of (I). If $x=y=z$, the second equation in (b) says that $(1+x)/|1+x|$ is a cube root of unity. This gives $\alpha=1$ and $x=(-1\pm i\sqrt{3})/2$, hence (2.23).

3. Spectral Properties

In this section we describe the spacing of eigenvalues, the ϕ dependence of energy bands and the location of eigenvalue crossings for networks with macroscopic components. The section is technical in character and prepares certain details that shall be needed later. It may be skipped by the uninterested reader.

A. *Density*

In the limit that the lengths of the macroscopic components of a network tend to ∞, there is a well-defined (integrated) density of states

$$\lim_{l\to\infty} \frac{(\#\text{ of states with } E<k^2/2m)}{l} = \frac{k}{\pi}, \tag{3.1}$$

where l is the total length of all the links. The density of states is a "property at infinity" and is not affected by the connectivity of the mesoscopic parts at all [31]. This is the reason why in an interval Δk of size $O(1)$ there are $O(l)$ states.

B. *Flat Bands*

The energy levels, $k_j(\boldsymbol{\phi})$, tend to be almost flat; that is, $k_j(\boldsymbol{\phi}) = k_j + O(l^{-1})$. Thus we can associate an essentially unique energy level, *independent of* $\boldsymbol{\phi}$, with a given energy.

This flatness can be understood as follows. Consider a network with the macroscopic components severed, as in Fig. 9. The spectrum of the disconnected network splits by component. The piece associated with a long lead has, of course, energy levels that are independent of $\boldsymbol{\phi}$. The piece associated with a long loop m has k-spectrum

$$\left\{ \left| \frac{2\pi n + \phi_m}{l} \right| \,\middle|\, n \in Z \right\}, \tag{3.2}$$

so the energy levels only vary in ϕ_m by $O(1/l)$. Only the mesoscopic part has energy levels that vary by $O(1)$. The three types of spectra are shown in Fig. 10.

For the connected system, by the Wigner–von Neuman no crossing rule, the combined spectrum will have levels that typically cross at isolated points in 3-flux space so each level is trapped in an interval of size $O(l^{-1})$.

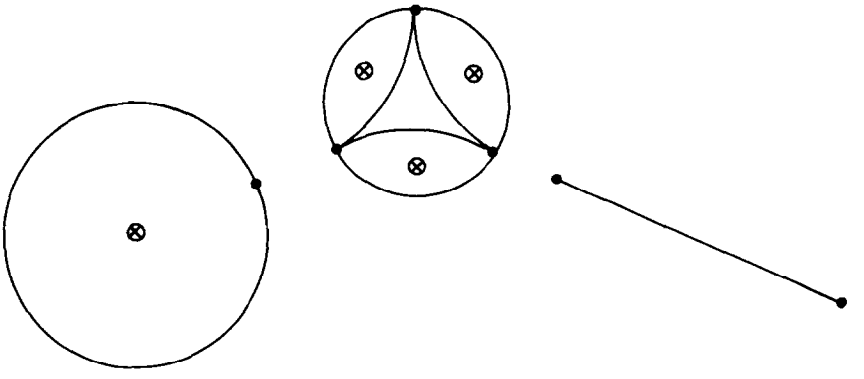

FIG. 9. A disconnected network with a mesoscopic part (the hubcap), a macroscopic loop, and a macroscopic lead.

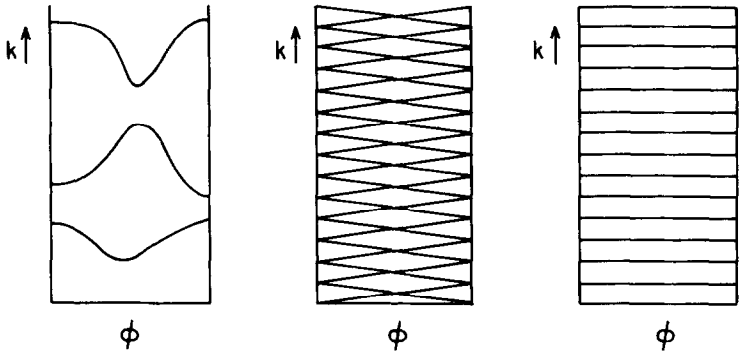

FIG. 10. The schematic spectra of the three components of the disconnected graph: (a) shows the mesoscopic spectrum; (b) the spectrum of the ring; (c) the spectrum of the lead.

C. *Adding a Lead*

The spectrum of a network with a lead is related to that without the lead. Assume that the lead is attached to the nth vertex and take $\lambda_{n+1} = 0$ for simplicity. N will denote the (mesoscopic) network, L the network with a lead attached, and R the reduced network with the nth vertex removed. Let $h_N(k, A)$ be the spectral matrix of N, $h_L(k, A)$ the spectral matrix of L and $h_R(k, A)$ the reduced spectral matrix obtained by deleting the nth row and nth column of h_N. By Eq. (2.17),

$$h_L = h_N + \tan(kl)\,|n\rangle\langle n|, \qquad |n\rangle \equiv (0, ..., 0, 1)^{\mathrm{T}}. \tag{3.3}$$

Expanding the determinants of h_L and h_N by minors on the last row we see that

$$\det(h_L) = \det(h_N) + \tan(kl)\det(h_R). \tag{3.4}$$

The eigenvalue equation is thus

$$\det(h_N) + \tan(kl)\det(h_R) = 0. \tag{3.5}$$

Assuming throughout that k is nonsingular, we have the following spectral information:

(i) *Away from the intersection of the spectra of N and R, the spectrum of the network with lead L is periodic in k with period π/l, up to corrections of $O(l^{-2})$, with one eigenvalue per period.*

(ii) *If k is an eigenvalue of N and R, then it is an eigenvalue of L, regardless of l.*

(iii) *Points in the spectrum of the mesoscopic network with multiplicity 2 or more are in the spectrum of the network with the lead attached as well.*

(iv) *If k is an eigenvalue for L with multiplicity two (or more), then k is an eigenvalue of both N and R.*

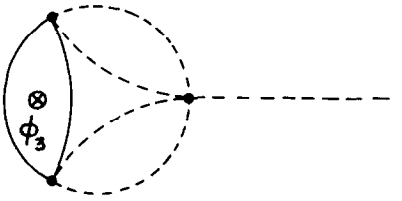

FIG. 11. The reduced graph associated to the hubcap with a macroscopic loop. The pieces that were removed from the graph are shown in broken lines.

The proof of these statements is: (i) The function $\tan(kl)$ is periodic in k with period π/l. Over one period the functions $\det h_N(k)$ and $\det h_R(k)$ change by $O(l^{-1})$, so, away from the spectrum of R, the ratio $\det h_N/\det h_R$ changes by $O(l^{-1})$, necessitating a mere $O(l^{-2})$ correction to the level spacing in $\tan(kl)$. Away from the spectrum of N we apply this argument to $\cot(kl)$ and $\det(h_R)/\det(h_N)$. Only at the intersection of the two spectra do both arguments break down. Finally, since $\tan(kl)$ is monotonic in each period, there is one eigenvalue per period. (ii) If $\det(h_N)=\det(h_R)=0$, then (3.5) is satisfied regardless of $\tan(kl)$. (iii) If k is an eigenvalue of N with multiplicity two or more, then h_N has corank 2 or more, and the rows of h_R must be linearly dependent, so k must be an eigenvalue of R. Now apply (ii). (iv) h_R is the reduction of h_L as well as that of h_N, so if h has corank 2 or more then h_R has determinant zero. By (3.4) this then implies that h_N has determinant zero.

EXAMPLE. The reduced network associated to the hubcap with a macroscopic lead is shown in Fig. 11 and has the spectral matrix

$$h_R(k, A) = [\sin(k)]^{-1} \begin{bmatrix} \alpha & 1+z \\ 1+\bar{z} & \alpha \end{bmatrix}, \tag{3.6}$$

whose spectrum is

$$\alpha = \pm 2\cos(\phi_3/2). \tag{3.7}$$

The set of points that satisfy Eq. (3.7) is a three-dimensional subspace of the $(k, \boldsymbol{\phi})$ cube that contains all the points of level crossings for h_L. A more detailed analysis that is carried out in Section 6 shows that the degeneracies actually lie on a subset of this made of two lines and three isolated points, see Fig. 12. However, just from Eq. (3.7) we conclude that the hubcap with a single lead attached has no level crossings, provided either $-4<\alpha<-2$ or $2<\alpha<4$. Also, with ϕ_3 fixed, level crossings occur only at the two energies given by Eq. (3.7).

D. *Adding as Many Leads as Vertices*

Adding leads of equal length to all vertices of a mesoscopic network is another case where the spectrum of the network with leads, L, with spectral matrix h_L, can

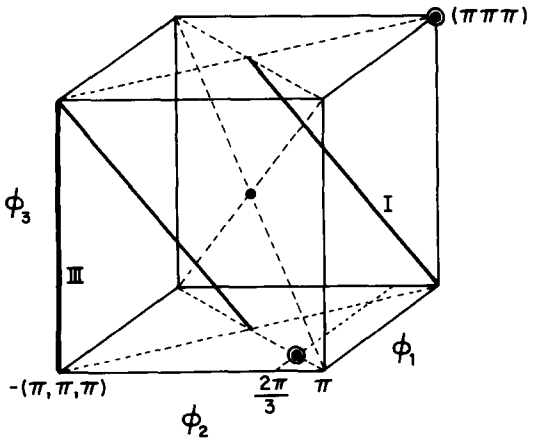

FIG. 12. The locus of level crossings in the flux cube for the hubcap with a macroscopic lead is shown as fat solid lines and fat dots. The dashed lines are to guide the eye only.

be understood by examining the spectral matrix h_N of the network with no leads, N. Taking, as usual, Neumann boundary conditions, we get from Eq. (2.17),

$$h_L(k, A) = h_N(k, A) + \tan(kl)I. \tag{3.8}$$

So, if we let $\zeta_1(k, \phi), ..., \zeta_n(k, \phi)$ be the n eigenvalues of $h_N(k)$,[1] then h_L will have determinant zero whenever

$$\tan(kl) + \zeta_j(k, \phi) = 0, \tag{3.9}$$

for some j. From Eqs. (3.8) and (3.9) we conclude that

> *The spectrum and zero vectors for L are both approximately periodic in k with period π/l, with n eigenvalues per period. Furthermore, in the $l \to \infty$ limit the eigenvalues for h_L cross for those ϕ's for which h_N is degenerate.*

With $O(1)$ vertices, h_N has, for fixed k, typically $O(1)$ level crossings. Thus, as $l \to \infty$, h_L has its crossings located on $O(1)$ smooth lines in the (k, ϕ) cube.

EXAMPLE. For the hubcap with three leads the locus of degeneracies are straight lines with ϕ fixed. They all lie on the body diagonal of the flux cube, $\phi_1 = \phi_2 = \phi_3$, and are shown in Fig. 13. There is a line of line of triple degeneracies at $\phi_1 = \pi$, and three lines of double degeneracy: two at $\phi_1 = \pm 2\pi/3$, and one at $\phi_1 = 0$. With l finite each line breaks so there is a point of degeneracy in each interval of size $\pi/l + O(l^{-2})$. For the line of triple degeneracies they are given by $\tan(kl) = 4\cot(k)$. Similar results holds for the lines of double degeneracies (see Fig. 14).

[1] Note that these are eigenvalues of the matrix at fixed k, not values of k for which the matrix has determinant zero.

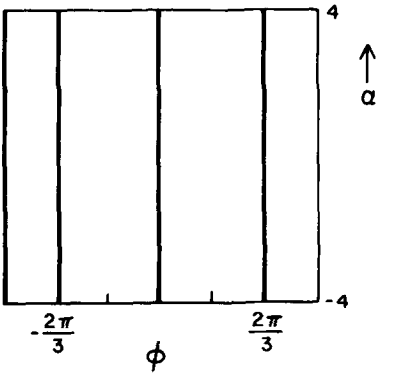

FIG. 13. The locus of level crossings in the (α, ϕ) square for the hubcap with a three macroscopic leads. ϕ is the coordinate on the body diagonal of the flux cube where all the degeneracies lie.

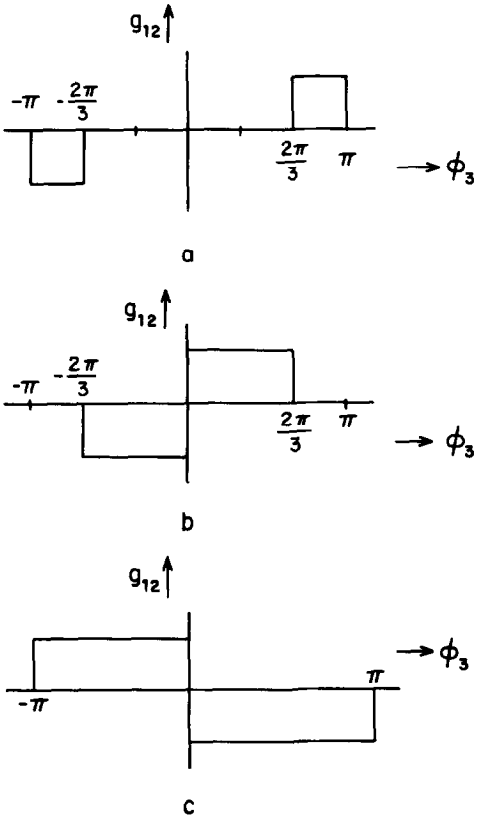

FIG. 14. The conductance graph of the mesoscopic hubcap: (a) for the ground state; (b) for the second state; (c) for the third state. The same set of graphs then repeats periodically in the state index. Each graph is periodic in the flux and one period only is shown. Note that the conductances of the three graphs sums to zero at each value of the controlling flux and that each graph is antisymmetric.

4. Charges

One basic technique for computing the Chern numbers relevant to conductances is to identify the points in flux space where the conductances jump and calculate the size of the jump. The points where the jumps occur are the points of level crossings. The size of the jump is the "charge" of the crossing. Our purpose in this chapter is to review the relation between these "charges" and the adiabatic conductances and describe in detail linearization techniques for computing the charges.

A. *Charges for Eigenvectors*

Consider a 3-flux Hamiltonian, $H(A)$, and let ϕ_0 be a point where two or more eigenvalues of H cross. Let $P_l(\phi)$ denote the spectral projection on the lth level (counting from below). Let

$$n_j = \mathrm{ch}(P_j, S^2(\phi_0)) \equiv \frac{i}{2\pi} \int_{S^2(\phi_0)} \mathrm{Tr}(P_j(dP_j)(dP_j)P_j) \tag{4.1}$$

be the Chern number of the jth spectral bundle on a small 2-sphere around ϕ_0.

We define the *charge* $q(\phi_0)$ to be the string of integers

$$q(\phi_0) = (n_1, n_2, \ldots). \tag{4.2}$$

This charge describes *all* the spectral bundles near ϕ_0. It is also convenient to define

$$Q(\phi_0) = (N_1, N_2, \ldots), \tag{4.3}$$

where

$$N_j = \sum_{k=1}^{j} n_k. \tag{4.4}$$

The basic properties of charges are:

(a) If the jth level is not degenerate at ϕ_0, then $n_j = 0$.

(b) $\sum_j n_j = 0$

(c) $q(\phi_0) = q(-\phi_0)$

(d) $\sum_\phi q(\phi) = 0$.

These properties are not hard to see. If the jth level is nondegenerate, P_j is smooth at ϕ_0, so S^2 is a boundary, and by Stokes' theorem the Chern number is zero. The sum over j of the Chern numbers n_j is the Chern number of the total bundle, which is trivial. (c) follows from time reversal symmetry. As for (d), the sum is the set of Chern numbers for all the levels on any surface enclosing all the charges. The boundary of the cube $[0, 2\pi]^3$ is such a surface. By periodicity, the abiabatic curvature is identical on opposite faces of this cube, and so it integrates to zero.

The numbers n_j are typically small integers. As will be shown in Section 8, one generically has

$$q(\boldsymbol{\phi}_0) = (0, ..., 0, \pm 1, \mp 1, 0, ..., 0). \tag{4.5}$$

Even with non-generic networks, we have not yet encountered an n_j bigger than 2.

The main use of the charges is to compute conductances. Let $g_{ij}(l, \phi_k)$ denote the quantized charge transport associated to the loops i and j, for level number l, as a function of the remaining flux ϕ_k, and let $\Sigma(\phi_k)$ be the planar section of the torus as in Fig. 15. Then, for $0 < \phi_k < \pi$,

$$\begin{aligned} g_{ij}(l, \phi_k) &\equiv \mathrm{ch}(P_l, \Sigma(\phi_k)) \\ &= \sum_{0 < (\phi_0)_k < \phi_k} n_l(\boldsymbol{\phi}_0) + \tfrac{1}{2} \sum_{(\phi_0)_k = 0} n_l(\boldsymbol{\phi}_0). \end{aligned} \tag{4.6}$$

This, together with the fact that $g_{ij}(l, \phi_k) = -g_{ij}(l, -\phi_k)$ allows us to compute the conductance for all values of ϕ_k (see [21] for details).

The advantage of computing quantized conductance via Equation (4.6), rather than as an explicit integral, is that the computation of charges is a local problem, requiring only perturbation theory near $\boldsymbol{\phi}_0$. As with all perturbation theory problems, computing the charges is easiest when the degeneracy is broken to first order in $\boldsymbol{\phi}$.

We therefore consider an N-fold level crossing, where the jth through $(N+j-1)$th levels cross, with the degeneracy broken to first order in $\boldsymbol{\phi}$. Linearizing around $\boldsymbol{\phi}_0$ we have $H(\boldsymbol{\phi}_0 + \delta\boldsymbol{\phi}) = 2H(\boldsymbol{\phi}_0) - H(\boldsymbol{\phi}_0 - \delta\boldsymbol{\phi})$, and so, for $0 \leqslant i < N$, $P_{j+i}(\boldsymbol{\phi}_0 + \delta\boldsymbol{\phi}) = P_{N+j-1-i}(\boldsymbol{\phi}_0 - \delta\boldsymbol{\phi})$. The map $\delta\boldsymbol{\phi} \to -\delta\boldsymbol{\phi}$ reverses orientation, and so

$$n_{j+i} = -n_{N+j-1-i}. \tag{4.7}$$

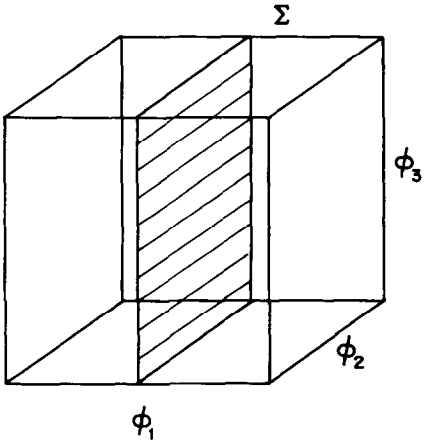

FIG. 15. The surface $\Sigma(\phi_1)$ that slices the flux torus.

We now specialize further to the case where the linearization looks like Berry's $\mathbf{J}\cdot\mathbf{B}$ example [32]. We suppose that, acting on the N-fold degenerate subspace, the linearization near $\boldsymbol{\phi}_0$ of the traceless part of H is given by

$$dH = \sum_{i,j=1}^{3} J_i M_{ij}\, d\phi_j, \tag{4.8}$$

where M is a non-singular 3×3 matrix and the J_i are a spin-J (irreducible) representation of the angular momentum algebra, with $N = 2J+1$. The matrix M maps the coordinates $\boldsymbol{\phi}$ to the coordinates $\mathbf{B}$ of Berry's example. This map is orientation preserving if $\det M > 0$ and orientation reversing if $\det M < 0$. We conclude that, for $0 \leqslant i \leqslant 2J$,

$$n_{j+i} = 2(i-J)\,\mathrm{sgn}(\det M). \tag{4.9}$$

For $N=2$, the linearization can always be written as (4.8), since the Pauli spin matrices span the 2×2 traceless Hermitian matrices. If the degeneracy is broken to first order, then $\det M \neq 0$ and the theorem applies. In this case Eq. (4.9) is due to [33].

For $N=3$, one might not expect the linearization often to take the form (4.8) with $J=1$, as the space of traceless 3×3 matrices is eight-dimensional. To see how this form *does* occur consider a 3-vertex network such that the flux ϕ_i is associated to a link connecting vertices j and k. The networks in Figs. 1–5 are of this form. See, e.g., Eq. (2.18) or (6.6). The linear variation with respect to the fluxes give three matrices that are proportional to

$$i\begin{bmatrix} 0 & 0 & 0 \\ 0 & 0 & x \\ 0 & -\bar{x} & 0 \end{bmatrix}, \quad i\begin{bmatrix} 0 & 0 & -\bar{y} \\ 0 & 0 & 0 \\ y & 0 & 0 \end{bmatrix}, \quad i\begin{bmatrix} 0 & z & 0 \\ -\bar{z} & 0 & 0 \\ 0 & 0 & 0 \end{bmatrix}, \tag{4.10}$$

where $x \equiv \exp(i\phi_1)$, etc. The three matrices (4.10) generate the spin-1 representation of the rotation group if $xyz = \pm 1$. So, provided the threefold degeneracy occurs on the planes $xyz = \pm 1$, the form (4.8) arises. When combined with the discussion of the next section this gives $q = (\pm 2, 0, \mp 2)$.

Alternatively, we may get a *reducible* spin-$\frac{1}{2}\oplus$spin-0 representation. If this breaks the degeneracy to first order, then the charge is $q = (\pm 1, 0, \mp 1)$. For the networks we have considered all linearizable 3-level crossings have proven to be of one of these two types.

For $N>3$ it is unlikely that dH would take the form (4.8), as there are many alternative mechanisms for breaking the degeneracy to first order.

B. *Charges for Zero Vectors*

Networks have special features that can be used to say additional things about the charges in general and can also be used to simplify computations. Consider a

network whose links have integer lengths and that have Neuman boundary conditions at the vertices ($\lambda_i = 0$). For such networks the spectral matrix is periodic in k with period 2π, so it is enough to consider the charges in the basic interval $k \in [0, 2\pi)$. We note also that the spectral matrix is odd in k, so $h(k, A)$ has the same kernel as $h(-k, A)$. This implies:

> *In a network with links of integer length and Neuman boundary conditions, the energy bands with $k \in (0, \pi)$ are in* 1-1 *correspondence with the energy bands with $k \in (\pi, 2\pi)$. Bands may touch, but not cross, the planes $k = 0$ or $k = \pi$. If there are a total of l bands with $k \in (0, 2\pi)$, then for any 2-surface S in flux space we have*
>
> $$\mathrm{ch}(P_j, S) = \mathrm{ch}(P_{l+1-j}, S). \tag{4.11}$$

In particular, at every level crossing we have $n_j = n_{l+1-j}$.

As a result, it is sufficient to consider the interval $k \in (0, \pi)$. We next develop formulas for the charges in terms of the spectral matrix $h(k, A)$ rather than the Hamiltonian $H(A)$.

Since the reduction from H to h breaks down when $\sin(kl_i) = 0$, we only consider the charges at level crossings where k does *not* take one of these special values. As before, we are mainly interested in systems where the degeneracies are split to first order in $\boldsymbol{\phi}$.

There are two important differences between H and h. First, h depends on four parameters $(k, \boldsymbol{\phi})$ rather the three parameters $\boldsymbol{\phi}$. Second, we are looking for zero vectors of h, not eigenvectors. As a result we need to consider all of h, not just the traceless part.

We therefore consider an N-fold level crossing, with $N = 2J + 1$ and with the degenerate levels numbered $j, j+1, \ldots, N+j-1$. We suppose that the linearization of h is

$$dh = \mathbf{x} \cdot \mathbf{J} + x_0,$$

$$x_\mu = \sum_{\nu=0}^{3} M_{\mu\nu}\, d\phi_\nu, \qquad \mu = 0, 1, 2, 3, \tag{4.12}$$

where M is a non-singular 4×4 real matrix, $d\phi_0$ means dk, and the J_i are a spin-J (irreducible, Hermitian) representation of the angular momentum algebra. Then for $0 \leqslant i \leqslant 2J$, we claim that

$$n_{j+i} = -2(i - J)\,\mathrm{sgn}(\det M). \tag{4.13}$$

To see this, first suppose that $M_{0j} = 0$, $j = 1, 2, 3$. The zero-vector problem then reduces to an eigenvector problem, with $-x_0$ being the eigenvalue. If $M_{00} < 0$ then the eigenvalue $-x_0$ is a positive multiple of dk, and Eq. (4.12) reduces to Eq. (4.8), and (4.13) follows. (Note that $\mathrm{sgn}(\det M) = \mathrm{sgn}(M_{00})\,\mathrm{sgn}(\det M_{ij})$, with M_{ij} the obvious 3×3 matrix). If $M_{00} > 0$ then the order of the eigenstates is reversed. By (4.5) this changes the sign of all the charges, and (4.13) still holds.

Now consider the general case, $M_{0i} \neq 0$; $\det h = 0$ when $|x_0| = m|\mathbf{x}|$, $m = -J, -J+1, ..., J$. This gives x-space a structure similar to Minkowski space, with the speed of light replaced by $|m|^{-1}$. Since there are precisely N solutions to the original Schrödinger equation for *every* value of $\boldsymbol{\phi}$, the transformation M that sends $(dk, d\boldsymbol{\phi})$ to $(x_0, \mathbf{x})$ must preserve the light-cones structure. In particular, M can be deformed into a matrix with $M_{0i} = M_{i0} = 0$ preserving

$$\operatorname{sgn}(\det M) = \operatorname{sgn}(M_{00}) \operatorname{sgn}(\det M_{ij}),$$

and preserving the charges.

5. The Hubcap—Charge Analysis

In this section we study the spectral properties, charges, and the Chern numbers associated to a mesoscopic network with as many long leads as vertices. In particular, we study in detail the hubcap with three long leads. As a prelude to this analysis we discuss the mesoscopic hubcap with no leads.

A. *The Mesoscopic Hubcap*

The general mesoscopic hubcap is parametrized by six lengths of the edges and three vertex potentials, and mesoscopic means that all lengths are $O(1)$.

With links of equal lengths (one, in appropriate units), and Neumann boundary conditions, the analysis simplifies in two ways. First, the system is periodic in k with period 2π. By the analysis of Section 4 it then suffices to consider $k \in (0, \pi]$, since all the Chern numbers are even functions of k. Second, the reduction from the Schrödinger equation to a matrix problem breaks down whenever $\sin(kl_{ij}) = 0$ for *any* link. Here, this only occurs at $k \equiv 0 \pmod{\pi}$.

This is not without a price. The hubcap exhibits symmetry when $\phi_1 = \phi_2 = \phi_3$, which leads to non-generic behavior (such as the presence of three-fold level crossings). This may make it difficult to appreciate what is special and what is general. For this reason we discuss generic behavior in Section 8.

Collecting the results about the spectral analysis from Section 2F and the appendix we have (see also Fig. 8):

> *For all $\boldsymbol{\phi} \neq 0$, there are three energy bands $k_j(\boldsymbol{\phi})$, $j = 1, 2, 3$ with $k_j \in (0, \pi)$. These bands cross at four points in the $(k, \boldsymbol{\phi})$ cube, all on the body diagonal $\phi_1 = \phi_2 = \phi_3$. There is a triple degeneracy at $\phi_i = \pi$, the upper two levels cross at $\phi_i = 0$, and the lower two levels cross at $\phi_i = \pm 2\pi/3$. In addition there is a flat band that is threefold degenerate for $k = n\pi$.*

We next compute the charges for $k \in (0, \pi)$. Since all level crossings lie on the body diagonal $\phi_1 = \phi_2 = \phi_3$, we label the points by this single value. From the basic properties of charges we know that $q(2\pi/3) = q(-2\pi/3) = (n_1, -n_1, 0)$ for some

integer n_1 and that $q(0) = (0, n_2, -n_2)$ for some integer n_2. Since the sum of all the charges must be zero, $q(\pi)$ must equal $(-2n_1, 2n_1 - n_2, n_2)$. So if we can compute $q(\pi)$ the other charges come for free.

Near $\phi = (\pi, \pi, \pi)$, dh is of the form (4.10), with $xyz = -1$. Equations (4.8) and (4.9) then apply, with $\operatorname{sgn}(\det M) = \operatorname{sgn}(\sin(k)) = 1$, and we conclude that $q(\pi) = (-2, 0, 2)$. This means that $n_1 = 1$ and $n_2 = 2$.

To sum up, for $k \in (0, \pi)$, the charges for the hubcap are

$$\begin{aligned} q(2\pi/3) = q(-2\pi/3) &= (1, -1, 0) \\ q(0) &= (0, 2, -2) \\ q(\pi) &= (-2, 0, 2). \end{aligned} \tag{5.1}$$

Using Eq. (4.4) we can now compute $g_{12}(j, \phi_3)$, the averaged conductance (i.e., Chern numbers), associated to loops 1 and 2 for the jth, band:

$$\begin{aligned} g_{12}(1, \phi_3) &= \begin{cases} 0 & \text{for } 0 < \phi_3 < 2\pi/3; \\ 1 & \text{for } 2\pi/3 < \phi_3 < \pi. \end{cases} \\ g_{12}(2, \phi_3) &= \begin{cases} 1 & \text{for } 0 < \phi_3 < 2\pi/3; \\ 0 & \text{for } 2\pi/3 < \phi_3 < \pi. \end{cases} \\ g_{12}(3, \phi_3) &= -1 \qquad \text{for } 0 < \phi_3 < \pi. \end{aligned} \tag{5.2}$$

These conductances are shown in Fig. 14. Cyclic permutations give g_{23} and g_{31}.

B. *The Hubcap with Three Leads*

With three leads of length l attached to the three vertices, Fig. 3, the spectral matrix is still given by Eq. (2.18), only now with

$$\alpha \equiv -4\cos(k) + \sin(k)\tan(kl). \tag{5.3}$$

Since $d\alpha/dk$ is always positive for $0 < k < \pi$ and $l > 1$, this amounts to a rescaling of the k-axis with basic period $O(1/l)$ instead of $O(1)$. The analysis of the previous section carries over and Eqs. (5.1)–(5.2) still hold. We can therefore translate the results for the mesoscopic hubcap to this case:

> *The hubcap with three leads of length l attached to the three vertices has its charges on the body diagonal $\phi_1 = \phi_2 = \phi_3$, repeating periodically with period* 3, *and are the same as the charges without leads. Namely,*

$$\begin{aligned} Q(\pm 2\pi/3) &= (1, 0, 0, 1, 0, 0, 1, \ldots) \\ Q(0) &= (0, 2, 0, 0, 2, 0, 0, \ldots) \\ Q(\pi) &= (-2, -2, 0, -2, -2, 0, -2, \ldots). \end{aligned} \tag{5.4}$$

Note that we choose to display the Q charges rather than the q charges.

The limit $l \to \infty$ has nice lines of degeneracies in (k, ϕ) space, as discussed in Section 3D. However the charge distribution on these lines does not have a nice limit. For example, for $\phi = 2\pi/3$ the line of degeneracies is made of three interlacing lines of charges, two neutral and one with charge one. This is characteristic to the *real scenario* that we now proceed to describe.

C. *The Real Scenario*

The real scenario occurs for networks with as many leads as vertices, in particular, for the hubcap with three leads. First, we want to note that the results of the previous section generalize. Indeed, by Section 3D the zero bundle for the network with leads corresponds to the eigenbundles for the spectral matrix with no leads. These are approximately periodic in k with period π/l, and there are as many states as vertices in each period. Networks whose vertices have a fixed valence (i.e., the same number of links attached to each vertex) have the additional special property that $h(k, \phi)$ takes the form $\tilde{h}(\phi) + \alpha(k)$, for some function $\alpha(k)$. As a result, the eigenbundles have the same structure as the zero bundles. In these cases, the (zero vector) Chern numbers of the network with leads are a repetition of the (zero vector) Chern numbers of the network without leads.

The periodic repetition of Chern numbers on small energy scales can lead to real (i.e., non-integer) transport. Let $p_j \equiv (1 + \exp[\beta(k_j^2 - k_F^2)/2m])^{-1}$ be the Fermi–Dirac occupation probability for the jth state. We are interested in temperature ranges that are small on energy scale of $O(1)$ but large on the scale of $O(1/l)$, i.e., $\pi^2/ml^2 \ll \beta^{-1} \ll \pi^2/m$. Take $0 < k_F < \pi$. The averaged conductance of noninteracting electrons $\langle g_{12} \rangle(\phi_3, \beta, k_F)$ is given by

$$\langle g_{12} \rangle(\phi_3, \beta, k_F) \equiv \sum_j p_j g_{12}(j, \phi_3). \tag{5.5}$$

Consider, for example, any three-vertex network. The Chern number of the $(3n+i)$th state is the same as that of the ith state. We can then write Eq. (5.5) as

$$\begin{aligned} \langle g_{12} \rangle(\phi_3, \beta, k_F) &= \sum_n [g_{12}(1, \phi_3)(p_{3n+1} - p_{3n+3}) + g_{12}(2, \phi_3)(p_{3n+2} - p_{3n+3})] \\ &= g_{12}(1, \phi_3)\, \omega_{13}(\phi_3, \beta, k_F) + g_{12}(2, \phi_3)\, \omega_{23}(\phi_3, \beta, k_F), \end{aligned} \tag{5.6}$$

where

$$\omega_{13}(\phi_3, \beta, k_F) \equiv \sum_n (p_{3n+1} - p_{3n+3}), \tag{5.7}$$

with a similar equation for $\omega_{23}(\phi_3, \beta, k_F)$. The $\omega_{ij}(\phi_3, \beta, k_F)$ are (real) weights with $0 < \omega_{23} < \omega_{13} < 1$. They have well-defined limits as $l \to \infty$ and $T \to 0$. The limiting conductances depend on ϕ_3 and k_F through both the Chern numbers and the weights. As the conductances are not quantized there is no reason for plateaus.

However, there are still discontinuities because the Chern numbers have integer jumps as ϕ_3 varies.

In particular, for the hubcap with three leads the Chern numbers are given in Eq. (5.2) and so the 1–2 conductance is bounded by 1 and is discontinuous at $\phi_3 = 0, \pm 2\pi/3$:

$$\langle g_{12} \rangle(\phi_3, k_F) = \begin{cases} \omega_{23}(\phi_3, \beta, k_F) & \text{for } 0 < \phi_3 < 2\pi/3; \\ \omega_{13}(\phi_3, \beta, k_F) & \text{for } 2\pi/3 < \phi_3 < \pi, \end{cases} \tag{5.8}$$

To sum up, in the real scenario a finite fraction of the states have non-zero Chern numbers. The Chern numbers come in n-tuples where n is the number of vertices and the Chern numbers of each n-tuple add to zero. The average conductance obtains a contribution only from the slight difference in occupation probability of the states *near the Fermi energy*. Summing over n-tuples gives the *non*-integer conductance. In this scenario the only thing that survives from the analogy to the Hall effect are the sharp jumps in the conductance as the "controlling" flux is varied. These jumps are separated on scale of $O(1)$.

6. Sections

A. *Sections, Singular Sets and Degrees*

An alternate method of calculating Chern numbers is to stay away from level crossings and focus on the zeroes of fields of eigenfunctions. To each zero we associate an integer valued degree, analogous to the integer charges associated with level crossings. This is similar to the approach of [34].

For a given energy level, $k_l(\boldsymbol{\phi})$, with the associated smooth projection $P_l(\boldsymbol{\phi})$, we are interested in the spectral bundle associated to the surface

$$\Sigma(\phi_i) = \{\phi_i, \phi_j, \phi_k \mid 0 \leqslant \phi_j, \phi_k \leqslant 2\pi\}, \tag{6.1}$$

(see Fig. 15), and in the associated Chern numbers $g_{jk}(\phi_i, l)$, where i, j, and k are cyclic permutations of 1, 2, 3. $\Sigma(\phi_i)$ must, of course, avoid crossings of the lth level.

A *section* V of the bundle is a smooth map from Σ to the bundle, sending each point $\boldsymbol{\phi}$ into the range of $P_l(\boldsymbol{\phi})$. In other words, V is a field of (unnormalized) eigenfunctions on Σ.

It is a basic fact (see, e.g., [35]) that if V fails to vanish on Σ, then the bundle over Σ is trivial and the associated Chern number vanishes. If V has isolated zeroes on Σ, then, by the Hopf degree formula (which we recall below), the Chern number is the sum of the degrees of the zeroes.

HOPF DEGREE FORMULA. *Let $\Sigma(\phi_k)$ be a planar slice of the 3-torus of fluxes, and let V be a section of the spectral bundle. Suppose that V has isolated zeroes on $\Sigma(\phi_k)$.*

Then the Chern numbers $g_{ij}(\phi_k)$ are given by the sum of integers

$$g_{ij}(\phi_k) = \sum_{\text{zeroes}} n_{m,k}, \tag{6.2}$$

$$n_{m,k} \equiv \int_{\gamma_m} \frac{1}{2\pi \|V\|^2} \operatorname{Im}\langle V \mid dV \rangle. \tag{6.3}$$

where γ_m is an oriented loop on $\Sigma(\phi_k)$ around the mth zero.

The degree (6.3) is the winding number of $V/\|V\|$ around the mth zero. If a section is defined on the entire $\boldsymbol{\phi}$-space and has isolated zeroes in that space, then we can assign three degrees to each zero, one for $\Sigma(\phi_1)$, one for $\Sigma(\phi_2)$, and one for $\Sigma(\phi_3)$.

It is especially easy to compute the degree if $\operatorname{Im}\langle \partial_i V \mid \partial_j V \rangle \neq 0$. In that case dV is nondegenerate, since for any direction (α, β) on Σ we have $\alpha\, \partial_i V + \beta\, \partial_j V \neq 0$. We can then linearize around the zero and perform the integral (6.3) directly on a small circle, obtaining

$$n_{m,k} = \operatorname{sgn} \operatorname{Im}\langle \partial_i V \mid \partial_j V \rangle. \tag{6.4}$$

The analysis of Chern numbers via sections cannot completely avoid analysis of degeneracies, since the spectral bundle is defined only for surfaces Σ that avoid level crossings. What *is* avoided is the analysis of charges.

The nice thing about our network problems is that, given the spectral matrix $h(k, A)$, one can easily find a section $V(k, \boldsymbol{\phi})$, once k is chosen to be a band function. To each vertex m in an n vertex network, we associate a vector-valued function $V_m(k, \boldsymbol{\phi})$, which is the vector of minors of h with respect to the mth row (equivalently, the n-dimensional cross product of the other $n-1$ rows). From the definition it follows that V_m is orthogonal to all but the mth row of h and that V_m dotted into the mth row gives $\det h$. In other words,

$$(hV_m)_j = (\det h)\, \delta_{jm}. \tag{6.5}$$

$V_m(k, \boldsymbol{\phi})$ is defined for all k; however, if $k(\boldsymbol{\phi})$ is a band function, $\det h(k(\boldsymbol{\phi}), \boldsymbol{\phi}) = 0$, and so $V_m(k(\boldsymbol{\phi}), \boldsymbol{\phi})$ is a section.

We call the set of points in $(k, \boldsymbol{\phi})$ space, where $V_m(k, \boldsymbol{\phi})$ vanishes the *singular set with respect to the mth vertex*. The singular set depends, of course, on m. In practice one tries to choose a distinguished vertex m that makes it as simple as possible.

The singular sets convey spectral information on the energy bands and on level crossings. Indeed, if $V_m = 0$, then by Eq. (6.5) $\det h = 0$. Furthermore, at level crossings h has rank at most $n-2$, so the cross product of *any* $n-1$ rows must vanish. We therefore conclude that:

(1) *Each singular set is contained in the spectrum.*

(2) *Points of level crossings are contained in each singular set. Indeed, they are the* intersection *of the singular sets with respect to all the vertices.*

B. *The Hubcap with a Macroscopic Lead*

For the hubcap with one long lead, Fig. 2, the spectral matrix is

$$h(k, A) = -\frac{1}{\sin(k)} \begin{bmatrix} \alpha & 1+z & 1+\bar{y} \\ 1+\bar{z} & \alpha & 1+x \\ 1+y & 1+\bar{x} & \alpha+\beta \end{bmatrix}$$
$$x \equiv \exp(i\phi_1), \qquad y \equiv \exp(i\phi_2), \qquad z \equiv \exp(i\phi_3), \tag{6.6}$$
$$\alpha \equiv -4\cos(k), \qquad \beta \equiv \sin(k)\tan(kl),$$

and as usual it is sufficient to consider $k \in (0, \pi)$. We shall call E, k, and α energies as they differ only be scaling. It is convenient to take l to be an odd integer. This is because if l is odd there are no triple degeneracies. (This can be seen as follows: At a triple degeneracy $h=0$, which requires $x=y=z=-1$, $\alpha=\beta=0$. β *is* zero when $\alpha=0$ for l even, but is not for l odd).

The hubcap with a long lead has a distinguished vertex, namely vertex 3, where the lead is attached. $V_3(k, \phi)$ is given by

$$V_3(k, \phi) = ((1+x)(1+z)-\alpha(1+\bar{y}), (1+\bar{y})(1+\bar{z})-\alpha(1+x), \alpha^2-|1+z|^2). \tag{6.7}$$

We consider the singular set with respect to this distinguished vertex. V_3 vanishes when

$$\alpha^2 = |1+z|^2, \qquad \alpha\,|1+x|^2 = \alpha\,|1+y|^2 = (1+x)(1+y)(1+z). \tag{6.8}$$

This occurs on three one-dimensional pieces ("strings") and one two-dimensional sheet in the (α, ϕ) cube, see Fig. 16. The strings are

$$\begin{aligned} &\text{I:} && x = y,\ z = x^{-2},\ \alpha = x + \bar{x}, \\ &\text{II:} && x = \bar{y},\ z = 1,\ \alpha = 2, \\ &\text{III:} && x = y = -1,\ \alpha = \pm 2\cos(\phi_3/2) \end{aligned} \tag{6.9}$$

and the sheet is

$$z = -1, \qquad \alpha = 0. \tag{6.10}$$

The sheet and string III obviously satisfy Eqs. (6.8). It remains to consider the case where the second equation is not just $0=0$. Note that

$$(1+x)(1+y)(1+z) = \pm 8(xyz)^{1/2} \prod_{j=1}^{3} \cos(\phi_j/2). \tag{6.11}$$

Since α is real, we conclude that either the second equation of (6.8) is trivial or

$$xyz = 1. \tag{6.12}$$

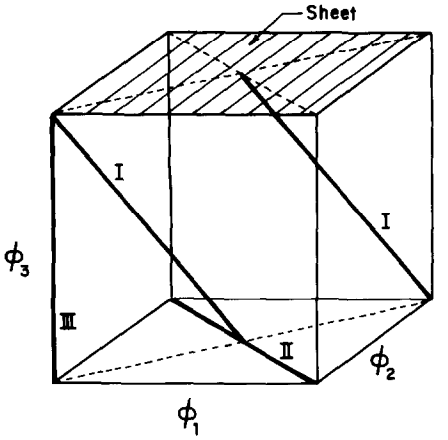

FIG. 16. The flux cube showing the singular set for the hubcap with a macroscopic lead, which is made of three straight lines (=strings), denoted by I, II, and III and a sheet. The dashed lines are to guide the eye only.

Also, if $\alpha \neq 0$ we have $|1+x| = |1+y|$, implying either $x = y$ or $x = \bar{y}$. These alternatives, together with (6.12), give strings I and II, respectively.

As noted above points of level crossing must lie on the singular set. They must also lie on the singular set with respect to the other two vertices. This gives the additional requirements

$$\alpha(\alpha+\beta) = |1+x|^2 = |1+y|^2. \tag{6.13}$$

This identifies the set of level crossings as follows:

The set of level crossings is made of three isolated points at

$$\phi_1 = -\phi_2 = \pm 2\pi/3,\ \phi_3 = \pi,\ \alpha = 2 \tag{6.14}$$

and

$$\phi_1 = \phi_2 = \phi_3 = \pi,\ \alpha = 0. \tag{6.15}$$

In addition there are $O(l)$ points of crossings, spaced $O(1/l)$ apart, that are located on the strings I and III of Eq. (6.9), *see Fig.* 12.

The first two points result from imposing Eq. (6.13) on string II, the third from imposing it on the sheet.

We are now ready to show that most energy levels are associated with trivial bundles (i.e., have zero Chern numbers, i.e., do not conduct). Fix an energy level near k and fix the "controlling" flux $\phi_3 \neq 0, \pi$. $\Sigma(\phi_3)$ avoids the singular set with respect to vertex 3 if

$$\alpha \neq \pm 2\cos(\phi_3/2). \tag{6.16}$$

Thus $V_3(k, \boldsymbol{\phi})$ has no zeroes on $\Sigma(\phi_3)$, and so the bundle has Chern number zero. This is the case for most k's. With ϕ_3 fixed, there can be only few conducting levels,

namely, those k for which (6.16) fails, so that $\Sigma(\phi_3)$ can intersect the singular set. (Such k's automatically lie on an energy band.) Of course, $\Sigma(\phi_3)$ must still avoid the set of degeneracies for the Chern number to be defined. As the latter set is discrete (as long as l is finite) by twiddling ϕ_3 we can avoid it without falling off the singular set.

It is actually nicer to consider the total conductance of all levels below the Fermi energy. The reason is that the associated spectral bundle is well defined even when levels below the Fermi energy cross. Therefore, the associated conductance, $g_{ij}(k_F, \phi_k)$, is an integer as long as inequality (6.16) holds at k_F. The procedure is to sum the Chern numbers for all energies less than k_F. The state responsible for the conductance would then be the state with $k < k_F$ for which (6.16) fails. This conducting state can lie deeply, i.e., $O(1)$, below the Fermi energ. It also follows that there are wide, i.e., $O(1)$, plateaus.

Similarly, with fixed k_F and fixed $\phi_1 \neq 0, \pi$ the g_{23} conductance is well defined if

$$2\cos(k_F) \neq -\cos(\phi_1). \tag{6.17}$$

This is the condition for $\Sigma(\phi_1)$ to avoid the level crossings that accumulate on string I.

It remains to determine the actual values of the integer conductances. For this we need to compute the three degrees (n_1, n_2, n_3) for each zero, as in (6.3). By direct computation

$$\begin{aligned}
\partial_1 V_3 &= (ix(1+z), -i\alpha x, 0) + \partial_1\alpha(-(1+\bar{y}), -(1+x), 2\alpha) \\
\partial_2 V_3 &= (i\alpha\bar{y}, -i\bar{y}(1+\bar{z}), 0) + \partial_2\alpha(-(1+\bar{y}), -(1+x), 2\alpha) \\
\partial_3 V_3 &= (iz(1+\bar{x}), -i\bar{z}(1+\bar{y}), i(z-\bar{z})) + \partial_3\alpha(-(1+\bar{y}), -(1+x), 2\alpha).
\end{aligned} \tag{6.18}$$

Using (6.8) we then find

$$\begin{aligned}
\operatorname{Im}\langle \partial_2 V_3 \mid \partial_3 V_3 \rangle &= \alpha^2 \operatorname{Im} y \\
\operatorname{Im}\langle \partial_3 V_3 \mid \partial_1 V_3 \rangle &= \alpha^2 \operatorname{Im} x \\
\operatorname{Im}\langle \partial_1 V_3 \mid \partial_2 V_3 \rangle &= 2\operatorname{Im}(\alpha\bar{x}\bar{y}(1+\bar{z})),
\end{aligned} \tag{6.19}$$

and so

$$\begin{aligned}
n_1 &\equiv \operatorname{sgn}\operatorname{Im}\langle \partial_2 V_3 \mid \partial_3 V_3 \rangle = \operatorname{sgn}(\sin(\phi_2)) \\
n_2 &\equiv \operatorname{sgn}\operatorname{Im}\langle \partial_3 V_3 \mid \partial_1 V_3 \rangle = \operatorname{sgn}(\sin(\phi_1)) \\
n_3 &\equiv \operatorname{sgn}\operatorname{Im}\langle \partial_1 V_3 \mid \partial_2 V_3 \rangle = -\operatorname{sgn}(\alpha(\sin(\phi_1+\phi_2)+\sin(\phi_1+\phi_2+\phi_3))).
\end{aligned} \tag{6.20}$$

Applying this to each string we conclude that

$$(n_1, n_2, n_3) = \begin{cases} \operatorname{sgn}(\sin(\phi_1))(1, 1, -1) & \text{on string I} \\ \operatorname{sgn}(\sin(\phi_1))(-1, 1, 0) & \text{on string II} \\ \operatorname{sgn}(-\alpha\sin(\phi_3))(0, 0, 1) & \text{on string III.} \end{cases} \tag{6.21}$$

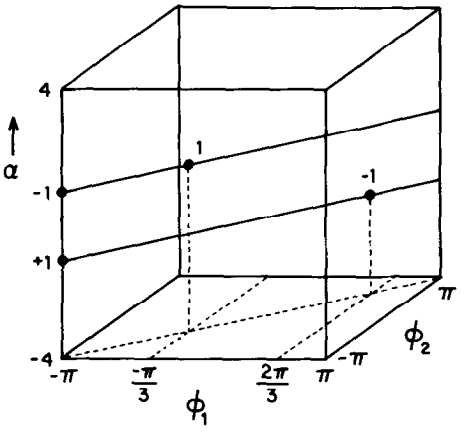

FIG. 17. A cross section of the (α, ϕ) cube with $\phi_3 = 2\pi/3$ showing the singular set for the hubcap with a macroscopic lead. The set is made of four points at two different energies. Two fixed energy levels are shown as solid lines. The total charge at each energy vanishes. The dashed lines are to guide the eye.

Remark. Because of symmetry this example is pathological in that the zeroes on the sheet are not isolated, and so we cannot compute their degrees. As we shall show later this behavior is not generic.

Figure 17 shows the (α, ϕ_1, ϕ_2) cube for fixed $\phi_3 = 2\pi/3$. Since $z \neq \pm 1$, string II of (6.7) and the sheet (6.8) do not contribute, and all zeroes have $\phi_1 = \phi_2$. The zeroes at the edges of the cube, $\phi_1 = \pi$ come from string III of (6.7), while the other zeroes come from string I. From (6.21) $+1$ and -1 degrees occur in pairs at the same energy, so we conclude that

$$g_{12}(k, \phi_3) = 0. \tag{6.22}$$

Summing over $k < k_F$ gives total conductance

$$g_{12}(k_F, \phi_3) = 0. \tag{6.23}$$

The (α, ϕ_2, ϕ_3) cube with fixed $\phi_1 = \pi/3$ is shown in Fig. 18. The solid line at $\alpha = 0$ comes from the sheet (6.8). We cannot associate a degree to this line but, as we shall see, we can avoid the difficulty this creates at the fixed energy $\alpha = 0$. The zero with degree -1 comes from string I and the zero at $\phi_3 = 0$ with degree $+1$ comes from string II.

Since the degrees plus the contribution of the singular line must add up to zero, the singular line cannot contribute anything.[2] We conclude that for $\pi < \phi_1 < 3\pi/2$,

$$g_{23}(\phi_1, k_F) = \begin{cases} 0 & \alpha > 2 \text{ or } \alpha < 2\cos(\phi_1) \\ -1 & \text{otherwise.} \end{cases} \tag{6.24}$$

[2] Under a generic perturbation of the system, the singular line breaks into an even number of discrete zeroes, half with degree $+1$ and half with degree -1.

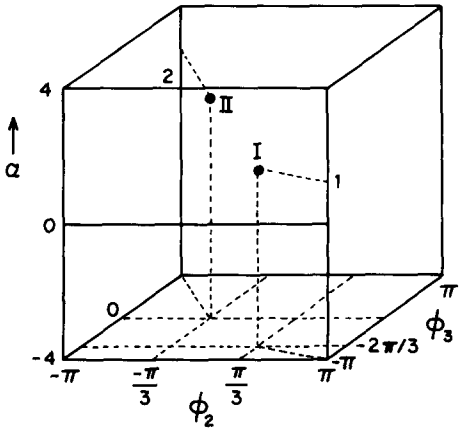

FIG. 18. The singular set in the (α, ϕ_2, ϕ_3) cube for ϕ_1 $\pi/3$, for the hubcap with a macroscopic lead. The set is made of two points and a line at $\alpha = 0$. The two points lie at different energies, and the charge of the cube is neutral. The dashed lines are to guide the eye.

The other ranges of ϕ_1 may be analyzed similarly and similar formulas result. Equations (6.23) and (6.24) are, of course, the main results of this subsection.

We have seen that the total conductance g_{23} is an integer-valued piecewise constant function of ϕ_1. However, *which* state is doing the conducting is (in the $l \to \infty$ limit) a *continuous* function of ϕ_1. There are $O(l)$ level crossings beneath the Fermi surface, and at each one the non-zero Chern number is passed along a string from one state to the next. The total conductance changes only when the Chern number is passed across the Fermi surface, i.e., when the Fermi surface intersects a string. Because there are very few non-zero Chern numbers which are passed around the $O(l)$ states, we call this the *bucket brigade* scenario.

C. *The Integer Scenario*

Consider a general n-vertex network with a long lead of length l attached to the nth vertex. $V_n(k, \boldsymbol{\phi})$, being a function of the *first* $n-1$ rows, does not depend on l. In particular, the singular set is independent of l, and has $O(1)$ components. As will be shown in Section 8, this set is generically one dimensional, composed of a number of strings. As l grows the energy bands are confined to intervals of size $O(l^{-1})$ in k. This says that $V_n(k, \boldsymbol{\phi})$ for k fixed is an approximate section for large l. The surface $\Sigma(\phi_3)$ would not intersect the singular set for most k's, giving zero Chern numbers to most levels. Only a few levels below the Fermi energy, $O(1)$, intersect with $\Sigma(\phi_3)$ and will conduct. As $l \to \infty$, the total number of states in any energy interval grows as $O(l)$, but the number of conducting states remains $O(1)$. The strings, being the solutions of trigonometric equations, are continuous and are dotted by points of level crossings. Thus, as ϕ_3 is varied, the non-zero Chern numbers are passed continuously from state to state along the string. This is the bucket brigade.

It follows that, even though the problem has a large parameter l and has $O(l)$ electrons, the conductance stays of order 1 and is affected only by $O(1)$ changes in the Fermi energy and the parameters.

The integer scenario has some of the interesting features of the integer Hall effect, which we now summarise:

(a) *There are wide plateaus of quantized, integer valued, conductances.*

(b) *The plateaus are separated by sharp integer jumps.*

(c) *The conductances are* $O(1)$.

(d) *The conducting states are few and may lie deep below the Fermi energy.*

7. Networks with a Macroscopic Loop

In this section we study the Chern numbers for mesoscopic networks with a macroscopic loop, such as Fig. 4. Two different physical settings are when the macroscopic loop is used to drive the system and when it is used to control it. Namely, if φ_i is the flux through the macroscopic loop, $g_{ij}(\phi_k)$ describes macroscopic driving while $g_{jk}(\phi_i)$ describes macroscopic control. As we shall see these give rise to different scenarios.

As in the rest of this work we address the questions: How can one compute the many Chern numbers that arise with macroscopic components? When is the average charge transport quantized to be an integer? When does one get the real scenario and when the integer scenario?

A. *The Hubcap with a Macroscopic Loop*

We consider the mesoscopic hubcap with unit links and one macroscopic loop, of length l an odd integer, enclosing flux ϕ_1. We look for level crossings and their charges[3] in order to compute the Chern numbers.

The 3×3 spectral matrix associated with this network is

$$h(k, A) = -\begin{bmatrix} \alpha & \dfrac{1+z}{s} & \dfrac{1+\bar{y}}{s} \\ \dfrac{1+\bar{z}}{s} & \alpha' & \dfrac{1}{s}+\dfrac{x}{s'} \\ \dfrac{1+y}{s} & \dfrac{1}{s}+\dfrac{\bar{x}}{s'} & \alpha' \end{bmatrix}, \tag{7.1}$$

where, as usual,

$$x \equiv \exp(i\phi_1), \qquad y \equiv \exp(i\phi_2), \qquad z \equiv \exp(i\phi_3). \tag{7.2}$$

[3] For a two-level crossing, the charge $q = (0, ..., 0, n, -n, 0, ...)$ depends on a single integer n. We will frequently use the term "charge" to means the single number n, rather than the complete sequence q. If Eq. (4.13) applies, then this charge is $n = \mathrm{sgn}(\det(M))$.

We use the menemonic

$$c \equiv \cos(k), \qquad s \equiv \sin(k), \qquad c' \equiv \cos(kl), \qquad s' \equiv \cos(kl), \qquad c_3 \equiv \cos(\phi_3), \tag{7.3}$$

and let

$$\alpha \equiv -4c/s, \qquad \alpha' \equiv -3c/s - c'/s'. \tag{7.4}$$

As we shall see, there is one isolated point of triple degeneracy and two sets of one-dimensional strings with double degeneracies. One set of strings has $y = z$ and the other has $y = \bar{z}$. The two types meet at the triple degeneracy. The strings carry well-defined charges; i.e., sgn det M is constant on intervals of length $O(1)$ on the strings.

First we look for level crossings at the discrete set of energies $c = 0$. If $l \equiv 1 \pmod 4$, then $s' = s = \pm 1$, and there is a triple degeneracy at $x = y = z = -1$. If $l \equiv 3 \pmod 4$ then $s' = -s$ and there is a triple degeneracy at $-x = y = z = -1$. The linear variation at these points is

$$dh = \frac{1}{s'} J_x \, d\phi_1 + \frac{1}{s}(J_y \, d\phi_2 + J_z \, d\phi_3) + \begin{bmatrix} 4 & & \\ & 3+l & \\ & & 3+l \end{bmatrix} dk, \tag{7.5}$$

where $J_{x,y,z}$ are the spin-1 angular momentum matrices. By the results of Section 4, the charge is $\pm(2, 0, -2)$, the sign depending on the signs of s and s'.

We henceforth look for crossings at $c \neq 0$. If Ψ is a zero vector of h, then the first line of $h\Psi = 0$ implies

$$\Psi_1 = \frac{1+z}{4c}\Psi_2 + \frac{1+\bar{y}}{4c}\Psi_3. \tag{7.6}$$

Plugging this into the last two lines we obtain that $\tilde{h}\binom{\Psi_2}{\Psi_3} = 0$, where

$$\tilde{h} = \begin{bmatrix} \dfrac{|1+z|^2}{4sc} - \dfrac{3c}{s} - \dfrac{c'}{s'} & \dfrac{(1+\bar{z})(1+\bar{y})}{4sc} + \dfrac{1}{s} + \dfrac{x}{s'} \\ \dfrac{(1+y)(1+z)}{4sc} + \dfrac{1}{s} + \dfrac{\bar{x}}{s'} & \dfrac{|1+y|^2}{4sc} - \dfrac{3c}{s} - \dfrac{c'}{s'} \end{bmatrix}. \tag{7.7}$$

Before getting into the analysis of level crossings, let us consider the linear variation of $\tilde{h}$, which we need to compute the charges:

$$\begin{aligned} d\tilde{h} = {} & \frac{i}{s'}\begin{bmatrix} 0 & x \\ -\bar{x} & 0 \end{bmatrix} d\phi_1 + \frac{i}{4sc}\begin{bmatrix} 0 & -\bar{y}(1+\bar{z}) \\ y(1+z) & y-\bar{y} \end{bmatrix} d\phi_2 \\ & + \frac{i}{4sc}\begin{bmatrix} z-\bar{z} & -\bar{z}(1+\bar{y}) \\ z(1+y) & 0 \end{bmatrix} d\phi_3 + \frac{l}{(s')^2}\left\{\begin{bmatrix} 1 & x \\ \bar{x} & 1 \end{bmatrix} + O(l^{-1})\right\} dh. \end{aligned} \tag{7.8}$$

This determines the 4×4 matrix M of Section 4B, to leading order in l, to be

$$\begin{bmatrix} \dfrac{2l}{(s')^2} & 0 & \dfrac{i(y-\bar{y})}{4sc} & \dfrac{i(z-\bar{z})}{4sc} \\ \dfrac{-c'(x+\bar{x})l}{(s')^2} & \dfrac{i(x-\bar{x})}{s'} & \dfrac{i[y(1+z)-\bar{y}(1+\bar{z})]}{4sc} & \dfrac{i[z(1+y)-\bar{z}(1+\bar{y})]}{4sc} \\ \dfrac{-ic'(x-\bar{x})l}{(s')^2} & \dfrac{-(x+\bar{x})}{s'} & \dfrac{y(1+z)+\bar{y}(1+\bar{z})}{4sc} & \dfrac{z(1+y)+\bar{z}(1+\bar{y})}{4sc} \\ 0 & 0 & \dfrac{-i(y-\bar{y})}{4sc} & \dfrac{i(z-\bar{z})}{4sc} \end{bmatrix}. \tag{7.9}$$

The determinant of this matrix has the same sign of the determinant of

$$M' = \begin{bmatrix} 2 & 0 & i(y-\bar{y}) & i(z-\bar{z}) \\ -c'(x+\bar{x}) & i(x-\bar{x})/s' & i[y(1+z)-\bar{y}(1+\bar{z})] & i[z(1+y)-\bar{z}(1+\bar{y})] \\ -ic'(x-\bar{x}) & -(x+\bar{x})/s' & [y(1+z)+\bar{y}(1+\bar{z})] & [z(1+y)+\bar{z}(1+\bar{y})] \\ 0 & 0 & -i(y-\bar{y}) & i(z-\bar{z}) \end{bmatrix}. \tag{7.10}$$

Note that this matrix depends on s', so $\operatorname{sgn}(\det M')$ is a rapidly varying function of the energy. From this one may be tempted to conclude that the charges on the strings are rapidly oscillating and there is no nice limit as $l\to\infty$. As we shall see, this is not the case.

We now return to the search for level crossings. At a crossing, $\tilde{h}$ has corank 2; i.e., h is the zero matrix. As the two diagonal terms must be equal, we must have $|1+y|=|1+z|$, and so either $y=z$ or $y=\bar{z}$. We first analyze the easier case, $y=\bar{z}$.

If $y=\bar{z}$, then x must be real, so $\phi_1=0$ or π. Setting $\tilde{h}_{21}$ and $\tilde{h}_{11}$ equal to zero we obtain

$$s' = \frac{-2csx}{1+c_3+2c}, \qquad c' = s'\frac{1+c_3-6c^2}{2cs} = -x\frac{1+c_3-6c^2}{1+c_3+2c}, \tag{7.11}$$

where we have used the fact that $|1+z|^2 = 2+2c_3$. We may then eliminate s' and c' to get

$$1 = (s')^2+(c')^2 = \frac{4c^2s^2+(1+c_3-6c^2)^2}{(1+c_3+2c)^2}. \tag{7.12}$$

A bit of algebra then gives

$$c_3 = \frac{8c^3-3c-1}{3c+1}. \tag{7.13}$$

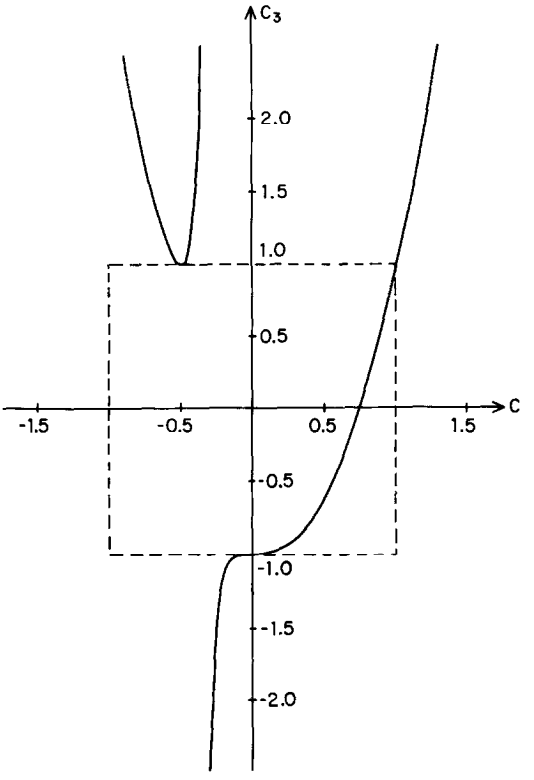

FIG. 19. The graph of Eq. (7.13) for the hubcap with a macroscopic loop carrying flux ϕ_1. The graph shows the locus of level crossings in the plane $(\cos(k), \cos(\phi_3))$ where the remaining coordinates are $y = \bar{z}$ and $x = \pm 1$.

Two other convenient forms for this expression are

$$c_3 = 1 + \frac{2(c-1)(2c+1)^2}{3c+1} = \frac{8c^3}{3c+1} - 1. \tag{7.14}$$

Of course, both c and c_3 must lie between -1 and $+1$. As shown in Fig. 19, there is an isolated solution at $c = -\frac{1}{2}$, $c_3 = 1$, and a continuum of solutions of $c \geqslant 0$, with c_3 going from -1 to $+1$ as c goes from 0 to 1. This gives the trajectory of a curve where the level crossings lie. (This curve in (c, c_3) space actually represents *two* curves in (k, ϕ) space, since $\phi_2 = -\phi_3$ may equal either $\pm\cos^{-1} c_3$).

However, level crossings do not occur at *every* point on this curve. s' is constrained by the relation $s' = \sin(l \sin^{-1}(s))$ (with a similar relation for c'). Since x may be chosen of either sign, this gives a level crossing every π/l along the curve (7.13). Since the spacing between levels is approximately π/l, this gives one

level crossing per gap along each piece of the trajectory (7.13). Of these, every other crossing is at $x=1$ (i.e., $\phi_1=0$), and the remaining ones are at $x=-1$ (i.e., $\phi_1=\pi$). The orientation-preserving approximate symmetry $k\to k+\pi/l$, $\phi_1\to\phi_1+\pi$ shows that all these crossings have the same charge and that the crossings at $x=-1$ are in precisely the gaps that alternate with the $x=+1$ crossings.

It remains to actually compute the charges. The expression (7.10) for M' simplifies with the substitutions $y=\bar{z}$ and $\bar{x}=x$. There is only one non-zero component in the second column. Adding the third column to the fourth column leaves only two non-zero components in the fourth column. Expanding by minors about the second and fourth rows we find

$$\begin{aligned}\det M' &= \frac{4ix(z-\bar{z})}{s'}\det\begin{bmatrix} 2 & -i(z-\bar{z}) \\ -2c'x & -i(z-\bar{z})\end{bmatrix} \\ &= -8x[i(z-\bar{z})]^2(1+c'x)/s'. \end{aligned} \tag{7.15}$$

By the first equation in (7.11) we know that s' and x have opposite signs for $c>0$,[4] so this expression is always positive, and *these charges are all* $+1$, *even though* sgn(det M) *is a rapidly oscillating function*!

We next consider the degeneracies with $y=z$. Setting $\tilde{h}_{21}=\tilde{h}_{11}=0$ gives

$$s'=\frac{-2cs\bar{x}}{z(1+c_3)+2c}, \qquad c'=s'\frac{1+c_3-6c^2}{2cs}=-\bar{x}\frac{1+c_3-6c^2}{z(1+c_3)+2c}, \tag{7.17}$$

where we have used the fact that $(1+z)^2=2z(1+c_3)$. Setting $|s'|^2+|c'|^2=1$, as before, gives

$$c_3^2+(1+3c)c_3+(3c-8c^3)=0, \tag{7.17}$$

or equivalently,

$$c_3=\frac{-1-3c\pm\sqrt{(1-3c)^2+32c^3}}{2}, \tag{7.18}$$

while ϕ_1 is given by

$$x=\frac{\pm|z(1+c_3)+2c|}{z(1+c_3)+2c}. \tag{7.19}$$

The graph of c_3 as function of c is shown in Fig. 20. Let γ be the real root of $(1-3\gamma)^2+32\gamma^3=0$ (γ is approximately -0.6262266). For $c<\gamma$ there are no solutions. For c between γ and 0, both roots of Eq. (7.18) lie between -1 and $+1$. For c between 0 and 1 only the plus branch is meaningful, and c_3 goes from 0 to 1 as

[4] Since $k\in(0,\pi)$, $s>0$. For k in $(\pi,2\pi)$, s', and x have the same sign and the charges are -1.

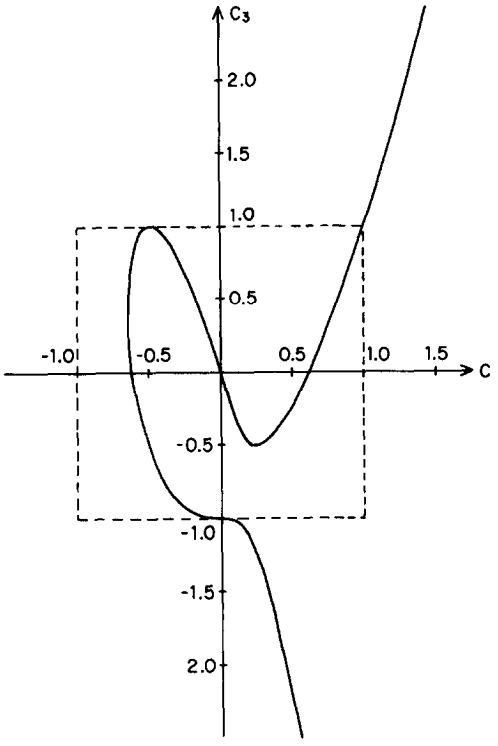

FIG. 20. The graph of Eq. (7.18) for the hubcap with a macroscopic loop carrying flux ϕ_1. The graph shows the locus of level crossings in the plane $(\cos(k), \cos(\phi_3))$, where the remaining coordinates are $y=z$ and x is determined by (7.19).

c goes from 0 to 1. For each of these solutions there are two values of $y=z$ that give rise to the same c_3 and c, namely $\phi_2=\phi_3=\pm\cos^{-1}(c_3)$.

As with the $y=\bar{z}$ crossings, x can take either of two values for any given value of c and z. Half the level crossings, filling every *other* gap, occur with x given by the plus sign in (7.19) while the other half, filling the remaining gaps, occur with x given by the minus sign in (7.19). The symmetry $k\to k+\pi/l$, $x\to -x$ interpolates between these two sets of degeneracies and shows that both have the same charge.

Let us compute this charge. Substitute $y=z$ into the expression (7.10) for M', and add the third column to the fourth column. This leaves only one non-zero component in the fourth column, so

$$\det M' = 2i(z-\bar{z})\det\begin{bmatrix} 2 & 0 & i(z-\bar{z}) \\ -c'(x+\bar{x}) & i(x-\bar{x})/s' & i[z(1+z)-\bar{z}(1+\bar{z})] \\ -ic'(x-\bar{x}) & -(x+\bar{x})/s' & z(1+z)+\bar{z}(1+\bar{z}) \end{bmatrix}$$

$$= 2i(z-\bar{z})[4i[xz(1+z)-\bar{x}\bar{z}(1+\bar{z})]/s' + 4ic'(z-\bar{z})/s']. \tag{7.20}$$

However, from Eq. (7.16) we know that

$$\frac{\bar{x}\bar{z}}{s'}=\frac{-(1+c_3+2c\bar{z})}{2cs}, \qquad \frac{xz}{s'}=\frac{-(1+c_3+2cz)}{2cs}, \qquad \frac{c'}{s'}=\frac{(1+c_3-6c^2)}{2cs}. \tag{7.21}$$

Plugging this into Eq. (7.20) we find that

$$\det M'=\frac{8(z-\bar{z})^2}{s}(3c+2c_3+1). \tag{7.22}$$

The first factor is always negative. By Eq. (7.18) the second factor is positive on the plus branch and negative on the minus branch.

Thus, for $k\in(0,\pi)$, the charges on the plus branch of the solution (7.18) are all -1, and the charges on the minus branch are all $+1$. This is consistent with the general theory of charges, which says that the sum over ϕ of the charges for a fixed energy level must be zero. For $c>0$ the $y=z$ charges (plus branch) balance the $y=\bar{z}$ charges. For $c<0$ the charges all come with $y=z$, and the plus branch balances the minus branch.

Finally, we consider the conductances. If the long loop is used to drive the network, i.e., we are looking at g_{12} or g_{13}, we have the bucket brigade, with a Chern number being passed along the strings (7.13) and (7.18), but with the peculiar feature that the crossings occur alternately at very different values of ϕ_1. For fixed $\phi_3\in(0,\pi)$, the total conductance g_{12} is -1 if $(\cos k_F, \cos\phi_3)$ is in the shaded region of Fig. 21, and zero otherwise. If, however, the macroscopic loop

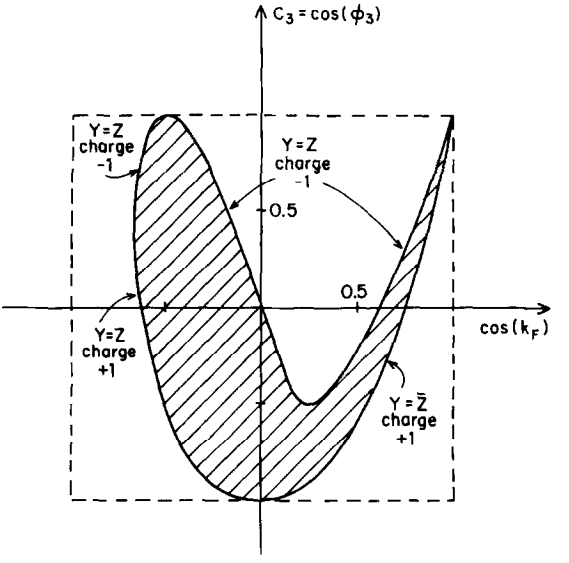

FIG. 21. The charges for the hubcap with a macroscopic loop and the region where $g_{12}(\phi_3)\neq 0$.

encloses the controlling flux; i.e., we look at g_{23}, then in any small range of x we only see charges in every *other* gap, giving us the real scenario. The g_{23} Chern number of a level depends on whether it lies just above or just below the relevant charge.

B. *General Networks with One Long Loop*

This general behavior may be expected in *any* network with one long loop of length l enclosing a flux ϕ_1. The contribution of this loop to the spectral matrix is to add $(-c'/s')$ to two of the diagonal entries and x/s' and $\bar{x}/s'$ to two off-diagonal entries. All these contributions are periodic in k with period $2\pi/l$ and are unchanged by the substitution $k \to k + \pi/l$, $x \to -x$. We expect pairs of lines of charges to form, with the symmetry interpolating between the two lines in a pair. Since the approximate level spacing is π/l, each line has a level crossing in every *other* gap, specifically in the gaps where the other line does *not* have level crossings. Because of the symmetry, the charges are the same on the two lines.

When we look at g_{13} or g_{23} we treat ϕ_1 as a free variable, and so we may identify the two lines of a pair. We then have one level clrossing par gap, all with the same charge, giving us the bucket brigade mechanism and the integer scenario. When we look at g_{23}, ϕ_1 is constrained and the two lines of each pair act separately, giving us the real scenario with period two.

If a long loop does not enclose any flux at all, then there is no automatic symmetry relating k and $k + \pi/l$, only one relating k and $k + 2\pi/l$. We thus expect to see the real scenario, with period two, for all three conductances. However, if the system possesses other symmetries, or if the charges cancel in a special way, it is possible to get the integer scenario for one or more of the conductances.

8. Generic Behavior

The explicit examples built around the hubcap are, of course, special. For example, we took all the mesoscopic links to have the same length, and there is a great deal of symmetry. As a result the examples (perhaps like all examples) are non-generic, and one would like to complement the information learned from them with the information available from the analysis of the generic situation. Such an analysis is presented here.

A. *Generic Rules and Codimensions*

In this section we consider generic spectral matrices $h(k, \boldsymbol{\phi})$. By this we mean that the family of Hermitian matrices obtained by letting k and $\boldsymbol{\phi}$ vary is embedded in the n^2-dimensional space of $n \times n$ Hermitian matrices in a "general position." If an event (say, $\det h = 0$) occurs in a codimension-1 set in the space of all Hermitian matrices, we assume it occurs in a codimension-1 set in the space of spectral matrices.

The first result concerns the frequency of level crossings and of zeroes of vector fields:

In the space of $n \times n$ Hermitian matrices,

(a) *The set of matrices with d-dimensional kernel (i.e., rank $n-d$) has codimension d^2.*

(b) *The set of matrices where the cross product of any $n-1$ rows vanishes (i.e., all the minors with respect to the remaining row vanish) has codimension 3.*

For 3-flux networks, part (a) says that level crossings occur generically at isolated points in (k, ϕ) space. Part (b) then says that singular sets with respect to any vertex are codimension 3, hence dimension-1 objects in the (k, ϕ) cube. A slice of fixed ϕ_i will therefore intersect the singular set at isolated points.

Note that we make no claims about how many (connected) components each set might have. In particular, with macroscopic components of length l the number of components can proliferate. This will be treated in the next section.

The proof runs as follows:

(a) is little more than the Wigner–von Neumann rules. A Hermitian matrix with corank d is determined by the $n-d$ non-zero eigenvalues, and by a diagonalizing $n \times n$ unitary matrix. The latter is unique up to an element of $U(d)(U(1))^{n-d}$, so

$$\begin{aligned} \dim(\ker d) &= n - d + \dim(U(n)) - \dim(U(d)) - \dim(U(1)^{n-d}) \\ &= n - d + n^2 - d^2 - (n-d) = n^2 - d^2. \end{aligned} \tag{8.1}$$

(b) Let h' be the $(n-1) \times n$ matrix made of the first $n-1$ rows of the $n \times n$ hermitian matrix h, and let h'' be the first $n-1$ columns of h'. We are interested in the set where h' had rank $n-2$ or less. For this to occur we first need h'' to have determinant zero, a codimension-1 event. If h'' has a rank $n-2$, we need the last column of h' to be linearly dependent on the columns of h''. (Alternatively, h'' may have rank $n-3$ or less, but by (a) that is already a codimension-4 event.) The component of the last column of h' in the direction orthogonal to the first $n-1$ columns must be zero. This event has complex codimension 1, or real codimension 2. Added to the codimension of $\det h' = 0$, this gives codimension 3.

Our second result concerns the distribution of charges among all possible 2-level crossings:

In the (n^2-4)-dimensional space of all possible 2-level crossings,

(a) *The charges ± 1 are generic. That is, they, and only they, occur on sets of codimension zero.*

(b) *Zero charges have codimension 1.*

(c) *All other possibilities have codimension 4 or more.*

This is seen as follows: Consider a 2-level crossing at a point (ϕ, k). Restrict the spectral matrix to the two-dimensional degenerate subspace, and linearize the problem in a neighborhood of (ϕ, k). The space of Hermitian 2×2 matrices is four-dimensional, and we have four parameters (ϕ, k). A 4×4 (real) matrix M_{ij} then maps $(d\phi, dk)$ to the components of dH.

If M_{ij} is invertible (the generic situation), then by Eq. (4.13) the charge is ± 1. If M instead has rank 3 (a codimension-1 event), we must use higher order perturbation theory to get the remaining component of dH as a function of a single variable, the zero vector of M. If this component is to lowest order an even function of this variable, then the charge is zero; if it is an odd function the charge is ± 1. For the charge to be anything other than $-1, 0, +1$, the matrix M would have to have rank 2 or less, a codimension-4 event.

Since by our first result threefold (or more) level crossings have codimension 5 relative to 2-level crossings, this second result is easily extended to *all* level crossings:

> *In the* (n^2-4)*-dimensional space of all possible level crossings, the charges* $q = (0, ..., 0, \pm 1, \mp 1, 0, ...)$ *are generic, the charge* $q = (0, 0, ...)$ *occurs with codimension* 1, *and all other possibilities have codimension* 4 *or more.*

B. *Degeneracies for Macroscopic Components*

For finite networks degeneracies occur at isolated points in the (k, ϕ) cube. However, as we have seen for the networks in the previous chapters, the number of degenerate points is $O(l)$ and in the limit $l \to \infty$ they coalesce to form $O(1)$ lines in the (k, ϕ) cube. We give here an alternate generic argument that shows why this is the case.

Macroscopic components that are all of the same length l, introduce into the spectral matrix the angle kl, which varies rapidly with k. The associated entries in the spectral matrix then run from $-\infty$ to $+\infty$ in intervals of k of order $O(1/l)$. Since the angle is practically independent of k we regard it as a free parameter. (The incommensurate case gives rise to several angles kl_i that can be viewed as independent parameters. This is, however, outside the scope of the present work.)

The rules in the previous section for counting the dimensions of various sets imply also that every free parameter reduces the codimension of an event by one. In particular with one free angle, level crossings are codimension 3 in the (k, ϕ) cube, i.e., are lines in the $l \to \infty$ limit. Because this takes care of the large parameter in the problem, one expects only $O(1)$ of them.

C. *The Two Scenarios*

The *real* and *integer* scenarios and the circumstances that lead to them can be understood heuristically as follows.

Consider the situation discussed in the previous section, where, in the $l \to \infty$ limit, points of level crossing accumulate on a line L. There are two possibilities.

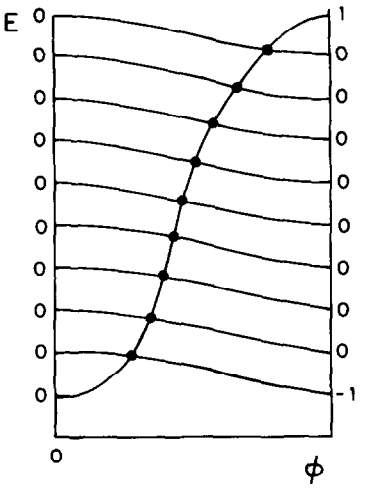

FIG. 22. Schematic energy bands diagram for a network with macroscopic components where the locus of degeneracies has eigenvalues of fixed multiplicity. This gives the bucket brigade scenario. The Chern numbers are all zero for zero controlling flux and for, say, $\phi = \pi/2$ have ± 1 separated by many zeroes.

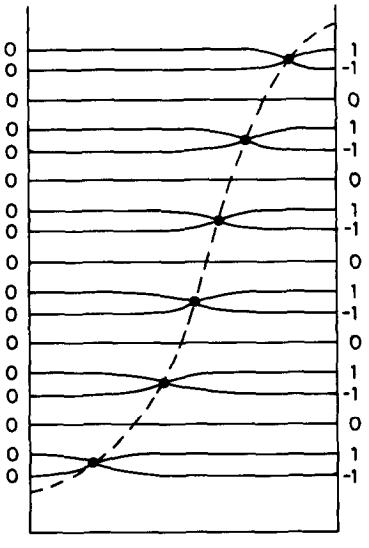

FIG. 23. A schematic energy bands diagram for a network with macroscopic components where the locus of degeneracies has eigenvalues of different multiplicities. Here crossings are pair creation events. The Chern numbers are all zero for zero controlling flux and turn to lots of 0, ± 1 for, say, $\phi = \pi/2$. This gives rise to the real scenario.

The simple case is when every pair of adjacent energy levels crosses on L, as shown in Fig. 22. The second and more complex case is when levels that do not enter level crossings are sandwiched between levels that do, as shown in Fig. 23.

One might expect the first possibility, in which states with similar energies behave similarly, to always occur. It does not, however, because states that are nearby in energy may not be nearby in other properties that are relevant for crossings, such as the support of the wave function. In a network with several macroscopic components there may well be states, supported largely on separate components, that have similar energies. We thus expect both situations to occur with frequency.

If L is simple, since each crossing has generically charge ± 1, we are in the *bucket brigade* situation where a unit of conductance is transported from one level to its immediate neigbor. There are only few levels that carry a unit of conductance for any fixed ϕ_i, and most of the levels are "insulating." This is the *integer scenario.*

On a complex L, however, the simple eigenvalues prevent the conductance from being passed up the line. Instead, each crossing can be viewed as a *pair creation* event. In this case, the levels associated to level crossings on L would carry say Chern number ± 1 while the levels associated to the simple eigenvalues would carry 0. As a consequence, a finite fraction have nontrivial Chern numbers. This is, of course, the *real scenario.*

9. Chern Numbers, Charge Transport and the Scattering Matrix

A. *The Scattering Matrix*

Until now we considered mesoscopic networks with macroscopic, but still finite, components. In this chapter we study mesoscopic networks with infinitely long leads directly. Such networks give rise to a natural scattering problem. On each lead there are incoming and outgoing amplitudes, related by

$$\Psi_{\text{out}} = S(k, A)\, \Psi_{\text{in}}. \tag{9.1}$$

Here Ψ_{in} is the m-vector of incoming amplitudes, Ψ_{out} is the vector of outgoing amplitudes. The scattering matrix $S(k, A)$ is a unitary $m \times m$ matrix, where m is the total number of modes in the leads. We consider single mode leads, so m equals the number of leads.

For example, a network with two leads, such as the network in Fig. 24, has a scattering matrix of the form

$$S = \begin{pmatrix} r & t^* z \\ t & -r^* z \end{pmatrix}, \qquad |t|^2 + |r|^2 = 1, \qquad |z| = 1, \tag{9.2}$$

where t and r are the reflection and transmission amplitudes.

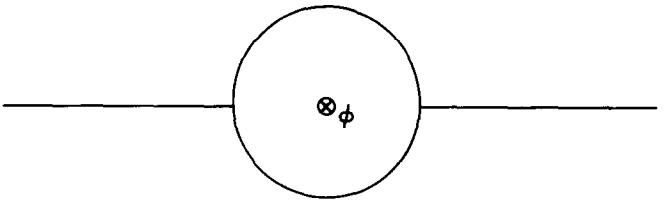

FIG. 24. A network with two leads connecting to a flux carrying ring.

It is natural to expect that the S matrix gives rise to a geometric theory of transport that parallels the geometric theory of transport for finite systems described in the preceding chapters. Such an expectation draws, in part, on ideas originally due to Landauer [36–38].

B. *Relation to the Special Matrix*

In this section we relate the scattering matrix S to the spectral matrix h of the networks *without* leads. This formula, Eq. (9.6) below, says that the scattering matrix can be read off almost directly from the graph.[5]

Consider an n-vertex network, Fig. 25, where m leads are attached to the first m vertices. Let Ψ_{in} and Ψ_{out} be the m-vectors of the amplitudes of the ingoing and outgoing waves on the leads. Then the n-vector of amplitudes on the vertices is

$$\Psi = (\Psi_{\text{in}} + \Psi_{\text{out}}, \Phi), \tag{9.3}$$

with Φ the $(n-m)$-vector of amplitudes on the remaining vertices.

The boundary conditions (2.2) now read

$$(kh)\Psi + ik(\Psi_{\text{out}} - \Psi_{\text{in}}, 0) = 0, \tag{9.4}$$

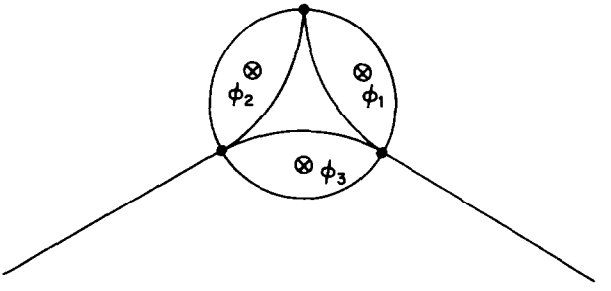

FIG. 25. The mesoscopic hubcap with two infinite leads.

[5] There are related results in [39, 40] where the scattering matrix for the graph is related to the scattering matrices of its components, i.e., the links and the vertices.

or, for $k \neq 0$,

$$(h + i\tilde{P})(\Psi_{\text{out}}, \Phi) = -(h - i\tilde{P})(\Psi_{\text{in}}, 0), \tag{9.5}$$

where $\tilde{P}$ is the projection onto the first m components of Ψ. From (9.5) follows:

The scattering matrix S is the $m \times m$ matrix

$$S = -\tilde{P}(h + i\tilde{P})^{-1}(h - i\tilde{P})\tilde{P}. \tag{9.6}$$

Remarks. (a) A particularly simple case is $n = m$, and $\tilde{P} = 1$. Then (9.6) simplifies to

$$S = -\frac{h - i}{h + i}. \tag{9.7}$$

S is manifestly unitary, being the Hilbert transform of the Hermitian matrix h. It also follows that

$$S^{\mathrm{T}}(k, A) = S(k, -A), \tag{9.8}$$

as one expects by time reversal (T = transpose). Furthermore, since h is Hermitian $(h + i)$ is always invertible (so long as k is nonsingular) and S inherits the smoothness of h. If $m < n$, however, this need not be the case, as we shall see below.

(b) In microwave theory there are similar formulas that relate the "voltage reflection coefficient" to the "normalized load impedance," see, e.g., [41].

(c) $S(k, A)$ and $S(k, A')$ with $\phi(A) - \phi(A') = 0 \mod 2\pi$ are related by a diagonal unitary matrix (a gauge transformation), just as $h(k, A)$ and $h(k, A')$ are. It follows that the diagonal entries of S are periodic in ϕ_i, while the off-diagonal entries have magnitudes that are periodic in ϕ_i, all with period 2π.

(d) $(h + i\tilde{P})$ fails to be invertible if and only if the network supports solutions that vanish on the m vertices where the leads are attached. These solutions are bound states that are embedded in the continuum. For points $(k, \boldsymbol{\phi})$ that support such states S can be singular. With $m = n$ an analogous thing can happen for singular k's. In potential scattering bound states embedded in the continuum are rare and require ingenious choices of the potentials [42]. Here, in contrast, such states are rather common.

(e) S is, of course, unitary, although this is not manifest in the expression (9.6). To see that $|\Psi_{\text{in}}| = |\Psi_{\text{out}}|$ for all Ψ_{in}, take (9.4) and left-multiply by $\Psi^{\dagger}$. The imaginary part of the resulting expression (which must equal zero) is k times $(|\Psi_{\text{out}}|^2 - |\Psi_{\text{in}}|^2)$.

C. *Examples*

As applications of Eq. (9.6), here we rederive results due to [43] that we derived independently but became aware of while this manuscript was being written. These examples were motivated by works on mesoscopic systems (see also [44, 45]).

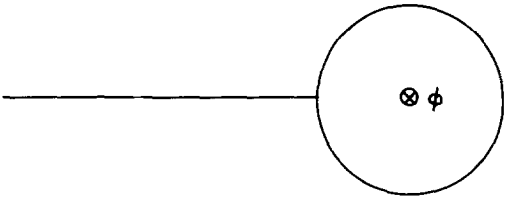

FIG. 26. A network with one lead connecting to a flux carrying ring.

EXAMPLE 9.1. For the network in Fig. 26 with $\lambda = 0$ and loop of unit length, the spectral matrix with the lead removed is, by (2.14), the function

$$h = -2\frac{\cos(k) - \cos(\phi)}{\sin(k)} \tag{9.9}$$

and the S matrix is the complex number

$$S = \frac{2[\cos(k) - \cos(\phi)] + i\sin(k)}{-2[\cos(k) - \cos(\phi)] + i\sin(k)}. \tag{9.10}$$

S lacks smoothness at the points

$$\sin(k) = 0, \qquad \cos(\phi) = \cos(k), \tag{9.11}$$

that is, when k is a multiple of π and $k + \phi$ is a multiple of 2π. For $\cos(\phi)$ fixed and near 1, the phase of S changes by 2π as $\sin(kl)$ passes through zero. This can be thought of as an example of Levinson's theorem in scattering theory [46], for at the values (9.11) of k and ϕ, the network supports a bound state on the loop that does not leak to the lead (see the Appendix for a discussion of singular loops).

Since ϕ, $\exp(ik)$, and S are all associated with the circle S^1, one can ask the degree of the maps $\phi \to S$ with k fixed and $k \to S$ with ϕ fixed. From (9.10) we see

$$\begin{aligned} \deg(k \to S) &= 2 \\ \deg(\phi \to S) &= 0. \end{aligned} \tag{9.12}$$

EXAMPLE 9.2. Consider the network in Fig. 24, where the two arcs each have unit length. The spectral matrix of the network with leads removed is

$$\begin{aligned} h &= (\sin(k))^{-1} \begin{pmatrix} -2\cos(k) & x + y \\ \bar{x} + \bar{y} & -2\cos(k) \end{pmatrix} \\ x &\equiv \exp(i\phi_1), \qquad y \equiv \exp(i\phi_2), \qquad x\bar{y} \equiv \exp(i\phi). \end{aligned} \tag{9.13}$$

From Eq. (9.7) we have

$$S = -\begin{pmatrix} -c-z & x+y \\ \bar{x}+\bar{y} & -c-z \end{pmatrix}\begin{pmatrix} -c-\bar{z} & x+y \\ \bar{x}+\bar{y} & -c-\bar{z} \end{pmatrix}^{-1}$$
$$= \frac{-1}{(c+\bar{z})^2 + |x+y|^2}\begin{pmatrix} |c+z|^2 - |x+y|^2 & (z-\bar{z})(x+y) \\ (z-\bar{z})(\bar{x}+\bar{y}) & |c+z|^2 - |x+y|^2 \end{pmatrix}, \tag{9.14}$$

where $c \equiv \cos(k)$ and $z \equiv \exp(ik)$. Note that, while S is not a function of the threading flux ϕ alone, the diagonal entries of S and the magnitudes of the off-diagonal entries are. (See Remark (b) of the previous section). As in the previous example, when the network supports a bound state that has no amplitude on the leads (i.e., $s=0$, $x=y$), S becomes singular. Using the Landauer formula, Eq. (9.17) below, the conductance of the network can be read from Eq. (9.14).

D. *Topological Questions*

Bound states are described by finite dimensional projections in $L^2(R^3)$ while scattering states are not. As a consequence the Chern numbers of scattering states when considered in $L^2(R^3)$ may be ill-defined. In fact, this is one of the reasons why the identification of the Chern numbers with adiabatic transport coefficients holds in generality only for finite systems [2].

In networks, however, scattering states *are* associated with finite dimensional projections in C^n ($n = \#$ of vertices), and one can study their Chern numbers. Something analogues to this occurs in the TKN^2 study [5, 7], where the Bloch states, once reduced to fixed quasimomentum, are associated to finite dimensional projections in L^2 (*Unit Cell*) with meaningful Chern numbers. As it turns out these Chern numbers are conductances as well.

In this section we describe, on a formal level, geometric objects and Chern numbers that are naturally associated with a scattering problem. In the next section we shall discuss their physical interpretation as transport coefficients.

Consider an n-vertex network with m leads attached to m vertices, and let $\tilde{P}$ be the projection onto these vertices. The eigenfunctions at fixed k are the solutions of

$$(1-\tilde{P})\, h(k, \phi)\, \Psi = 0. \tag{9.15}$$

The *bundle of scattering states* has as its fibers the vector spaces spanned by the solutions to Eq. (9.15) with (k, ϕ) fixed. The fiber has dimension

$$\operatorname{corank}[(1-\tilde{P})\, h(k, \phi)] \geqslant m. \tag{9.16}$$

For most k, h has full rank and so this dimension equals m. Thus the bundle of scattering states on m leads has m-dimensional fibers, as expected.

One can now ask two geometric questions. First, how is the bundle of scattering states embedded in C^n? Second, what are the Chern numbers associated to the eigenbundles of the scattering matrix considered as an m-dimensional unitary

matrix? The second question, in particular, is the obvious analog of questions asked about the eigenbundles of Hermitian Hamiltonians.

Two extreme situations are when the network has n leads and when it has a single lead. In the case of n leads the bundle of scattering states is trivial because the fibers span C^n. However, the n eigenstates of S can have n interesting Chern numbers. With a single lead the situation is in a sense reversed. The scattering matrix is a complex number and has only trivial eigenbundles. However, the one-dimensional fiber of scattering states can twist in C^n.

E. *Physical Interpretation*

The geometric questions of the preceding section suggest that there are interesting integers that one can associate with scattering problems for networks. It is, however, not clear from this discussion what their physical interpretation is. In particular, it is not clear that they have anything to do with charge transport.

There is another angle that suggests a connection between scattering and transport but which appears to have no topological content. This is the Landauer–Büttiker theory of quantum transport [36–38, 47]. See also [48] for a review. For a two-lead situation, the Landauer formula gives the conductance g in terms of the entries of the scattering matrix in (9.1):

$$g = |t|^2/|r|^2. \tag{9.17}$$

(The multimode case is more complicated.) This equation has no recognized topological content.[6] Also, the conductance in this formula and the adiabatic conductances of the preceding chapters are objects of rather different nature. Specifically, the first is associated with dissipation in systems coupled to baths and the latter is nondissipative in isolated systems. Nevertheless, there are reasons to believe that a geometric interpretation of the Landauer formula exists. For example, related formulas make contact with the Hall effect [50, 51].

Putting all this together suggests that the coefficients of adiabatic transport (that are known to be geometric) must be related to the Chern numbers associated with the scattering problem. In the following two sections we shall describe Chern–Landauer type formulas for networks with one and n leads.

F. *Networks with One Lead*

Consider an n-vertex networks with an infinite lead attached to the nth vertex. The scattering matrix is just a complex phase. Specializing Eq. (9.6) to the case where $\tilde{P}$ is rank one gives

$$S = -\frac{1 - i(h^{-1})_{nn}}{1 + i(h^{-1})_{nn}}. \tag{9.18}$$

[6] Anderson and Lee [49] relate g to phases of the transmission amplitude in the vein of the relations derived below for the adiabatic conductances.

Since S is one dimensional its eigenbundle is trivial. We can, however, ask how is the one-dimensional bundle of scattering states, the solutions of (9.16), embedded in $\mathbf{C}^n$. The vector $V_n(k, \phi)$ of Section 6 is a section of this bundle, since by Eq. (6.5) $(hV_n)_j$ is zero for $j \neq n$, regardless of k. Since the twisting of V_n determines the transport coefficients at energy k, we conclude that:

> *For a network with one infinitely long lead, the line bundle of scattering states with fixed energy has Chern numbers whose interpretation is the adiabatic transport coefficients at the energy k.*

G. *Networks with as Many Leads as Vertices*

If a lead is attached to each vertex, then the scattering matrix is given by Eq. (9.7). As a result, the eigenbundles of S are precisely the eigenbundles of h. In Section 5D we saw that the zero-vector bundles of a network with n equally large but finite leads were the eigenbundles of h. We therefore conclude that:

> *For fixed k, the n eigenbundles of the scattering matrix have n Chern numbers that correspond to the adiabatic charge transport of the n repeating eigenstates of the network with long but finite leads near the energy k.*

APPENDIX: The Spectral Matrix for Singular k

In this appendix we treat the exceptional cases of Section 2, where the ordinary construction of a spectral matrix breaks down. We treat the cases where a lead is singular (i.e., $\cot(kl) = -\lambda_{n+1}/k$), where a link is singular ($\sin(kl) = 0$), and where there are several singular links forming one or more loops.

A. *Singular Leads*

Consider a network with one singular lead attached to the nth vertex, i.e., a lead for which $\cot(kl) = -\lambda_{n+1}/k$. Equation (2.15) then cannot determine Ψ_{n+1}, but does set $\Psi_n = 0$. (If any *non*singular leads are attached to vertex n, this also implies that ψ is zero on these leads). Ψ_{n+1} can be determined from the boundary condition (2.2) applied at vertex n, and is

$$\Psi_{n+1} = -\sin(kl) \sum \frac{\Psi_j \exp(-i\phi_{jn})}{\sin(kl_{jn})}, \tag{A.1}$$

where the sum is over all links (but not nonsingular leads!) that connect to vertex n, where l_{jn} is the length of the link and ϕ_{jn} is the integrated vector potential along the link. The remaining $n-1$ amplitudes $(\Psi_1, ..., \Psi_{n-1})$ are determined by an $(n-1)$-dimensional matrix h_r, obtained from the n-dimensional spectral matrix by removing the nth row and the nth column. (The nth row has already been used to determine Ψ_{n+1}, and the nth column does not contribute because $\Psi_n = 0$).

If there are several (say m) singular leads attached to the nth vertex, then the analysis is as above with one exception. The boundary condition at n does not entirely determine the wave function on these leads, but merely provides one constraint to the m degrees of freedom. As a result there are $(m-1)$-independent solutions supported entirely on the singular leads.

Regardless of the number of leads, the reduced matrix can be associated to a reduced graph, as in Fig. 11. Delete the nth vertex and all links connected to the nth vertex, and introduce fictitious vertex potentials

$$\lambda_j = k \cot(kl_{jn}), \tag{A.2}$$

for all vertices j that connect to n. These results are summarized as follows:

Suppose several leads are attached to the nth vertex of a network, and suppose that k is such that $m \geqslant 1$ of these leads are singular. Construct h_r as above, by deleting the nth row and nth column of h. Then

(a) *If $m > 1$, or if* $\det h_r = 0$, *then k is in the spectrum with multipicity* $\operatorname{corank}(h_r) + (m-1)$. (*If $m = 1$ and h_r is invertible then k is not in the spectrum*).

(b) *There are exactly $(m-1)$ solutions supported entirely on the singular leads. That is, solutions with $(\Psi_1, ..., \Psi_n) = 0$.*

(c) *All solutions have $\Psi_n = 0$ and have $(\Psi_1, ..., \Psi_{n-1})$ in the kernel of h_r.*

B. *Singular Links*

Suppose that a singular link runs from vertex i to vertex j. That is, $\sin(kl_{ij}) = 0$. We call the link *even* if $\cos(kl_{ij}) = 1$ and *odd* if $\cos(kl_{ij}) = -1$. By a choice of gauge we can always assume that

$$\exp(i\phi(l_{ij}))\cos(kl_{ij}) = 1. \tag{A.3}$$

On a singular link the wave function is *not* determined by its values at the endpoints, since we can fit a sine wave with nodes at both endpoints. However, since the wavefunction must take the form

$$\psi(x) = \exp(i\phi(x))[A \sin(kx) + B \cos(kx)], \tag{A.4}$$

we see that $\Psi_i = \Psi_j$. Adding the i and j boundary conditions (2.2) gives

$$\sum_l D_l \psi = (\lambda_i + \lambda_j)\psi, \tag{A.5}$$

where the sum is over all links that emanate from either i or j. The singular link connecting i and j appears twice in this sum, with the two terms adding to zero.

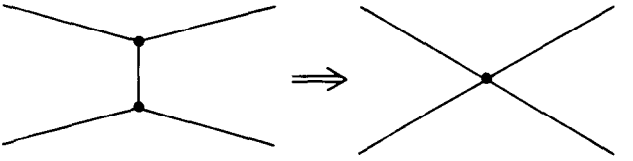

FIG. 27. Fusing vertices.

This is seen from

$$(D\psi)(x) = k \exp[i\phi(x)][A \cos(kx) - B \sin(kx)], \tag{A.6}$$

which gives $(D_l\psi)_i = -(D_l\psi)_j$ (the minus sign coming from the convention that derivatives be taken outwards along the links).

We can therefore treat i and j as a "fused" vertex, with boundary factor $\lambda_i + \lambda_j$. This is illustrated graphically in Fig. 27. In terms of matrices, identifying vertices i and j is the same as adding the ith and jth rows of the spectral matrix, and then adding the ith and jth columns, to form a new matrix of one less dimension. Repeating this procedure for each singular link, we get the following rule:

> *Suppose k is such that a network of n vertices has m singular links that do not close to form any loops. Form a reduced network of $n-m$ vertices by identifying vertices that are joined by singular links, and by then deleting the singular links. Let h_r be the spectral matrix of this reduced network. k is in the spectrum of the original network if and only* $\det h_r = 0$, *and the multiplicity of k is the corank of h_r.*

C. *Singular and Dangling Loops*

Suppose now that k is such that the singular links form a closed loop i. Since the flux ϕ_i through the loop is gauge invariant, the gauge choice (A.3) can typically be made for all but one singular link of a loop. The reduced network has the last singular link transformed into a singular dangling loop enclosing all of the flux ϕ_i (plus π if an odd number of odd singular links were remove); see Fig. 28.

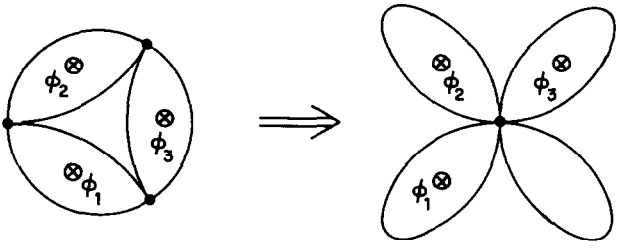

FIG. 28. Four dangling loops that result from fusion in the mesoscopic hubcap where all the links have the same length and so become simultaneously singular.

We must therefore consider how to treat a dangling singular loop, of length l, enclosing flux ϕ, attached to vertex n of an otherwise nonsingular network. The procedure depends on whether or not

$$\exp(i\phi) = \cos(kl). \tag{A.7}$$

This is equivalent to the original large loop satisfying

$$\exp(i\phi_i) = \cos(kl_i), \tag{A.8}$$

with l_i being the total length of the loop.

The simpler case is when equality does not hold. In that case the amplitude B of the cosine wave (A.6) on the loop must equal zero, as must Ψ_n, since $B = \Psi_n = B\cos(kl)\exp(i\phi)$. The amplitude A of the sine wave is determined by the boundary condition (2.2) at n. This is much like the case of a singular lead. We delete the nth vertex and all nonsingular leads and links attached to this vertex, adding the fictitious potentials (A.2). If $m > 1$ such loops are attached to vertex n, then there are $m-1$ bound states supported on the loops, consisting of sine waves whose derivatives at n add up to zero.

When (A.7) does hold, then $B = \Psi_n$ need not be zero, and A is not determined by other data. There exists a bound state supported entirely on the loop, with $A \neq 0$ and $\Psi_i = 0$ for all i. To find the other eigenstates, we delete the loop but not the vertex n, since Ψ_n need not be zero.

Combining these cases we get the rules:

Suppose k is such that there are l connected singular links, forming m loops and touching v vertices.

(a) *If all the loops satisfy* (A.8), *then there are exactly m solutions for which $\Psi_i = 0$ for all i. To find the solutions with nonzero Ψ_i, proceed as in Section B. Identify all the v vertices, but do not remove the (nonsingular) links connecting these vertices to the rest of the network. Form the reduced spectral matrix h_r for this reduced network. The number of solutions with ψ nonzero on the vertices is the corank of h_r.*

(b) *If at least one loop fails to satisfy* (A.8), *then there are exactly $m-1$ solutions with $\Psi_i = 0$ for all i, and all solutions have $\psi = 0$ on the v vertices touching the singular links. To get the reduced network, delete all v vertices, as well as all links touching these vertices, and form the resulting h_r. The number of solutions with ψ nonzero on the remaining vertices is the corank of h_r.*

Remarks. (a) If a network has singular links forming *disconnected* loops, then this reduction must be applied separately to each connected singular component.

(b) If we set $m = 0$, we recover the rules of Section B.

(c) If $m > 1$, then k is in the spectrum, with multiplicity at least $m-1$, regardless of the vector potential A. These "flat bands" solutions have a degeneracy that is stable under lots of deformations.

As an application, we consider the hubcap with links of unit lengths. The singular k's are $k = n\pi$, $n = 1, 1, \ldots$. Here $m = 4$, with three loops of length two and flux ϕ_i, and one loop of length three and flux zero.

First suppose that (A.8) is satisfied for each of the loops. This occurs only at the points $\phi = 0$, $k = 2n\pi$. Then there are $m = 4$ solutions with $\Psi = 0$ on the vertices. The reduced network consists of a single point with no links, so $h_r = 0$ has corank 1, and we have one more solution, for a total of five. This last mode corresponds to a solution that is non-zero and constant on the vertices.

At all points other than $\phi = 0$, $k = 2n\pi$, (A.8) fails for at least one loop. There are then $m - 1 = 3$ solutions with $\Psi = 0$ on the vertices. These are the only solutions, as the reduced network is empty. To sum up,

> *There are flat bands with a threefold degeneracy at the singular k's. At the special points $\phi = 0$, $k = 2n\pi$, the degeneracy is fivefold.*

REFERENCES

1. R. B. LAUGHLIN, *Phys. Rev. B* **23** (1981), 5632.
2. J. E. AVRON, R. SEILER, AND L. G. YAFFE, *Commun. Math. Phys.* **110** (1987), 33.
3. Q. NIU AND D. J. THOULESS, *Phys. Rev. B* **35** (1987), 2188.
4. M. KLEIN AND R. SEILER, Power law correction to the Kubo formula vanish in quantum Hall systems, Technical University Berlin preprint.
5. B. A. DUBROVIN AND S. P. NOVIKOV, *Sov. Phys. JETP* **52** (1980), 511.
6. S. P. NOVIKOV, *Sov. Math. Dokl.* **23** (1981), 298.
7. D. J. THOULESS, M. KOHMOTO, P. NIGHTINGALE, AND M. DEN NIJS, *Phys. Rev. Lett.* **49** (1982), 405.
8. D. J. THOULESS, *Phys. Rev. B* **27** (1983), 6083.
9. J. E. AVRON, R. SEILER, AND B. SIMON, *Phys. Rev. Lett.* **51** (1983), 51.
10. I. DANA, J. E. AVRON, AND J. ZAK, *J. Phys. C* **18** (1985), L679.
11. A. H. MCDONALD, *Phys. Rev. B* **29** (1984), 3057.
12. F. D. M. HALDANE, *Phys. Rev. Lett.* **55** (1985), 2095.
13. B. I. HALPERIN, *Japan J. Appl. Phys. Suppl.* **26** (1987), 1913.
14. M. KOHMOTO, *Ann Phys. (N.Y.)* **160** (1985), 343.
15. H. KUNZ, *Commun. Math. Phys.* **112** (1987), 121.
16. H. KUNZ, Adiabatic charge transport and topological invariants for electrons in a quasi-periodic potential and a magnetic field, EPFL preprint.
17. J. BELLISSARD, *in* "Localization in Disordered Systems" (W. Weller and P. Ziesche, Eds.), Texts in Physics, Teubner, Leipzig, 1988.
18. J. BELLISSARD, *in* "Operator Algebras and Applications, Vol. 2" (D. E. Evans and M. Takesaki, Eds.), Lecture Notes, Vol. 136, London Math. Soc., Cambridge, 1988.
19. G. MORANDI, "Quantum Hall Effect," Bibliopolis, Napoli, 1988.
20. J. XIA, *Commun. Math. Phys.* **119** (1988), 29.
21. J. E. AVRON, A. RAVEH, AND B. ZUR, *Rev. Mod. Phys.* **60** (1988), 873.
22. J. E. AVRON AND L. SADUN, *Phys. Rev. Lett.* **62** (1989), 3082.
23. Y. IMRY, *in* "Direction in Condensed Matter Physics" (G. Grinstein and G. Mazensko, Eds.), World Scientific, Singapore, 1986.

24. M. WILKINSON, *J. Phys. A* **20** (1987), 4337.
25. H. KUNZ, *Phys. Rev. Lett.* **57** (1986), 1095.
26. K. RUEDENBERY AND C. W. SCHERR, *J. Chem. Phys.* **21** (1953), 1565.
27. P. G. DE GENNES, *C.R. Acad. Sci. Ser. A* **292** (1981), 179.
28. S. ALEXANDER, *Phys. Rev. B* **27** (1983), 1541.
29. P. EXNER AND P. ŠEBA, Free quantum motion on a branching graph, Dubna preprint.
30. P. EXNER AND P. ŠEBA, *Phys. Lett. A* **128** (1988), 493.
31. H. L. CYCON, R. G. FROESE, W. KIRSCH, AND B. SIMON, "Schrödinger Operators with Application to Quantum Mechanics and Global Geometry," Springer-Verlag, New York/Berlin, 1986.
32. M. V. BERRY, *Proc. Roy. Soc. London A* **392** (1984), 45.
33. B. SIMON, *Phys. Rev. Lett.* **51** (1983), 2167.
34. D. P. AROVAS, R. N. BHATT, F. D. M. HALDANE, P. B. LITTLEWOOD, AND R. RAMMAL, *Phys. Rev. Lett.* **60** (1988), 619.
35. J. W. MILNOR AND J. D. STASHEFF, "Characteristic Classes," Princeton Univ. Press, Princeton, NJ, 1974.
36. R. LANDAUER, *IBM J. Res. Develop.* **1** (1957), 223.
37. R. LANDAUER, *IBM J. Res. Develop.* **32** (1986), 306.
38. M. BÜTTIKER, *Ann. N.Y. Acad. Sci.* **480** (1986), 194.
39. M. JEFFREY, C. GREEN, S. TYAGI, AND R. GILMORE, *Int. J. of Modern Phys. B* **2** (1988), 1399.
40. M. JEFFREY, C. GREEN, S. TYAGI, AND R. GILMORE, *Phys. Rev. B* **39** (1989), 9054.
41. A. TERRAS, "Harmonic Analysis on Symmetric Spaces and Applications," Springer-Verlag, New York/Berlin, 1985.
42. D. PEARSON, "Quantum Scattering and Spectral Theory," Academic Press, New York/London, 1988.
43. B. R. BULKA, *Z. Phys. B Condens. Matter Quanta* **1** (1989), 2217.
44. Y. GEFEN, Y. IMRY, AND M. YA. AZBEL, *Phys. Rev. Lett.* **52** (1984), 129.
45. M. BŰTTIKER, *Phys. Rev. B* **32** (1985), 1846.
46. J. R. TAYLOR, "Scattering Theory," Wiley, New York, 1972.
47. M. BÜTTIKER, Y. IMRY, R. LANDAUER, AND S. PINHAS, *Phys. Rev. B* **31** (1985), 6207.
48. A. D. STONE AND A. SZAFER, *IBM J. Res. Dev.* **32** (1988), 384.
49. P. W. ANDERSON AND P. LEE, *Suppl. Prog. Theor. Phys.* **69** (1980), 212.
50. P. STREDA, J. KUCERA, AND A. H. MACDONALD, *Phys. Rev. Lett.* **59** (1987), 1973.
51. J. K. JAIN AND S. A. KIVELSON, *Phys. Rev. B* **37** (1988), 4276.
52. N. I. GERASSIMENKO AND B. S. PAVLOV, *Acad. Nauk SSR Theor. Math. Phys.* **75** (1988), 187.
53. N. I. GERASSIMENKO, *Acad. Nauk SSR Theor. Math. Phys.* **74** (1988), 345.